博士論文

Discovery of novel immunosuppressive roles of intravenous immunoglobulin (IVIg)

（免疫グロブリン製剤（IVIg）が有する新たな免疫抑制作用の発見）

堀　采音

広島大学大学院先端物質科学研究科

2020 年 3 月

目次

1. 主論文

Discovery of novel immunosuppressive roles of intravenous immunoglobulin (IVIg)
(免疫グロブリン製剤 (IVIg) が有する新たな免疫抑制作用の発見)
堀　采音

2. 公表論文

(1) Anti-inflammatory intravenous immunoglobulin (IVIg) suppresses homeostatic proliferation of B cells
Ayane Hori, Takashi Fujimura, and Seiji Kawamoto
Cytotechnology, 70, 921-927 (2018).

(2) Intravenous immunoglobulin (IVIg) acts directly on conventional T cells to suppress T cell receptor signaling
Ayane Hori, Takashi Fujimura, Mai Murakami, Jungyeon Park, and Seiji Kawamoto
Biochemical and Biophysical Research Communications, 522, 792-798 (2020).

3. 参考論文

(1) Intake of a fermented plant product attenuates allergic symptoms without changing systemic immune responses in a mouse model of Japanese cedar pollinosis
Takashi Fujimura, Ayane Hori, Hideto Torii, Shinsuke Kishida, Yoshinori Matsuura, and Seiji Kawamoto
World Allergy Organization Journal, 11, 31-39 (2018).

主論文

Contents

General introduction

Chapter 1: Intravenous immunoglobulin (IVIg) acts directly on steady-state B cells to suppress their homeostatic expansion

1.1. Introduction

1.2. Materials and methods

1.2.1. Mice and ethical statement

1.2.2. Reagents

1.2.3. Purification or depletion of B and T cells from murine splenocytes

1.2.4. Cell labeling with fluorescent dye

1.2.5. Cell culture

1.2.6. Proliferation assay

1.2.7. Microscopic analysis

1.2.8. Neutralization of Fcγ receptors (CD16/32) and integrin β2 (CD18)

1.2.9. Statistical analysis

1.3. Results

1.3.1. IVIg suppresses proliferation of murine splenocytes in steady-state

1.3.2. IVIg suppresses homeostatic proliferation of B cells

1.3.3. IVIg induces B cell-specific aggregation

1.3.4. Fcγ receptors and integrin β2 are not involved in IVIg-mediated aggregation and suppression of homeostatic proliferation

1.4. Discussion

Chapter 2: IVIg acts directly on conventional T cells to suppress their activation upon T cell receptor (TCR) ligation

2.1. Introduction

2.2. Materials and methods

2.2.1. Mice and ethical statement

2.2.2. Reagents

2.2.3. Cultivation of splenocytes with immunostimulants

2.2.4. Flow cytometoric analysis of cell cycle arrest and apoptosis

2.2.5. Purification of T cells from murine splenocytes

2.2.6. T cell culture with phytohemagglutinin (PHA) or anti-CD3 antibody

2.2.7. Flow cytometoric analysis of regulatory T cells (Treg)

2.2.8. Analysis of cytokine production

2.2.9. IL-2 supplementation assay

2.2.10. Western blotting

2.2.11. Immunoprecipitation

2.2.12. nano LC-MS/MS analysis

2.2.13. Statistical analysis

2.3. Results

2.3.1. IVIg suppresses proliferation of splenocytes upon stimulation with T cell-tropic stimulants

2.3.2. IVIg induces G_1 cell cycle arrest of T cells, but does not induce apoptosis

2.3.3. IVIg suppresses proliferation of purified T cells upon TCR ligation

2.3.4. IVIg does not induce expansion of $CD4^+$ $Foxp3^+$ Treg

2.3.5. IVIg negatively regulates TCR signaling

2.4. Discussion

General conclusions

Acknowledgments

References

General introduction

Intravenous immunoglobulin (IVIg) therapy is the injection therapy of pooled human immunoglobulin derived from thousands of blood donation volunteers. The major component of IVIg agent is polyclonal immunoglobulin G (IgG) fraction prepared from human plasma [1], and a large amount of immunoglobulins (0.1-2 g/kg body mass) is administered to patients with autoimmune and severe infectious diseases [2].

The IVIg therapy has a long history. In 1890, von Behring firstly communicated serum application against diphtheria [3] and tetanus [4]. Since then, IVIg has been object of intense investigation in terms of function and clinical application [1]. Later, IVIg was tried to use for patients with primary antibody defiencies who developed chronic bacterial infections [5], and the first application of IVIg for autoimmune diseases was proposed in 1981 [6]. Nowadays, the therapeutic efficacy of IVIg is widely accepted. Indeed, the IVIg therapy adapts serious inflammatory diseases such as Kawasaki disease (KD), Guillain-Barre symdrome, idiopathic thrombocytopenic purpura (ITP), systemic lupus erythematosus (SLE), and chronic inflammatory demyelinating polyneuropathy (CIDP).

Autoimmune diseases are conditions elicited by abnormal immune responses to a normal body part, and many of them are accompanied by acute or chronic inflammation. Several autoimmune diseases are designated as intractable diseases in Japan, and their accurate mechanisms for pathogenesis and effective treatment are not completely established. Contemporary theories suggest that autoimmunity is the result of a multi-orchestrated immune response, and the overview of autoimmune progression is described in Fig. 1 [7]. The recognition of molecular mimicry, xenobiotics and autoantigen by antigen presenting cells (APC) including dendritic cells (DC), macrophages (MΦ), and natural killer cells (NK) lead to initiation of autoimmunity (Fig. 1A). The activated APC present antigenic peptides to uncommitted T helper (Th0) lymphocytes, which then differentiate into Th2, follicular helper (Tfh), Th17, Th1 or regulatory T cells (Treg) (Fig. 1B). B cells are activated by Tfh and Th2, and then become mature and differentiate into plasma cells, which produce autoantibodies (Fig. 1C). Through antibody-dependent cell-mediated cytotoxicity (ADCC), interaction with receptor of target cells and deposition of immune complex (IC), and autoantibodies may mediate autoimmune diseases (Fig. 1D). These autoimmune mechanisms *via* autoantibodies are observed in SLE [8], Sjogren's syndrome (SS) [9], and rheumatoid arthritis (RA) [10]. Increased Th17 provokes inflammation through secretion of

interleukin (IL)-17 in several autoimmune diseases such as RA [11], SLE [12], SS [13], and multiple sclerosis (MS) [14] (Fig. 1E). Th1 cells drive the development of cytotoxic T lymphocytes (CTL), which cause tissue injury by secretion of cytotoxic granules or cytokines (Fig. 1F). Cytotoxicity driven by Th1 is seen in type 1 diabetes (T1D) [15] and primary biliary cirrhosis (PBC) [16]. Decreased Treg, which negatively regulates both innate and adaptive immune responses, disturbs immune tolerance (Fig. 1G). Low level of Treg occurs in SLE [17], MS [18], and RA [19].

Treatment by using steroids or immunosuppressant is the major approach to treat autoimmune diseases as a symptomatic treatment. However, these treatments are not suitable for patients lacking physical strength such as children and after surgery, because normal immune responses are also impeded by steroids or immunosuppressant. IVIg is the alternative therapy for above cases, and moreover, it is vital for patients in acute phase of severe inflammation as a last-minute strategy. For example, IVIg is a representative therapy of KD, which is an acute self-limited vasculitis of unknown etiology that occurs predominantly in infants and young children [20]. The recommended therapy for all KD patients in the acute phase generally administers IVIg agent, 2 g/kg over 10-12 hours [21]. In the case of SLE, which is a multisystem autoimmune disease with diverse manifestation, some reports suggest that IVIg may be

beneficial and safe for various manifestations in mice model as well as in human patients [22,23] . Thus, the anti-inflammatory effects of IVIg are widely recognized in mouse models of inflammatory disorders and human clinical settings. However, the accurate mechanisms of IVIg remain to be elucidated.

To elucidate therapeutic mechanisms of IVIg is quite important in order to develop more effective and safer treatment techniques. Not only benefits, but IVIg therapy gives physical burden by high dose of immunoglobulin agent and long-time injection. In addition, it is a disadvantage that the risk of infection cannot be completely ruled out because IVIg agent derives from pooled human plasma. To solve these problems, it is necessary to develop molecular targeted drugs that mimic the therapeutic effects of IVIg. However, the creation of molecular targeted drugs is difficult under the current situation in which the therapeutic mechanisms of IVIg are not clear. Therefore, basic research to understand the therapeutic mechanisms of IVIg would play a part in the development of therapeutic techniques for the treatment of inflammatory diseases.

In this thesis, I aimed to redefine and elucidate the target cell subsets and immunosuppressive mechanisms of IVIg based on a hypothesis that IVIg fulfills its immunosuppressive activities through multiple cell targets and molecular mechanisms.

B cells and T cells play critical roles in the advance of inflammation (Fig. 1). Thus, I focused on the immunosuppressive effects of IVIg on B cells and T cells. In chapter 1, I tried to reveal immunosuppressive role of IVIg on steady-satate B cells. In chapter 2, I attempted to elucidate immunosuppressive effect of IVIg on activated T cells. The present results would provide new insight into exploration of valuable drug targets on the treatment of chronic and acute inflammatory disorders.

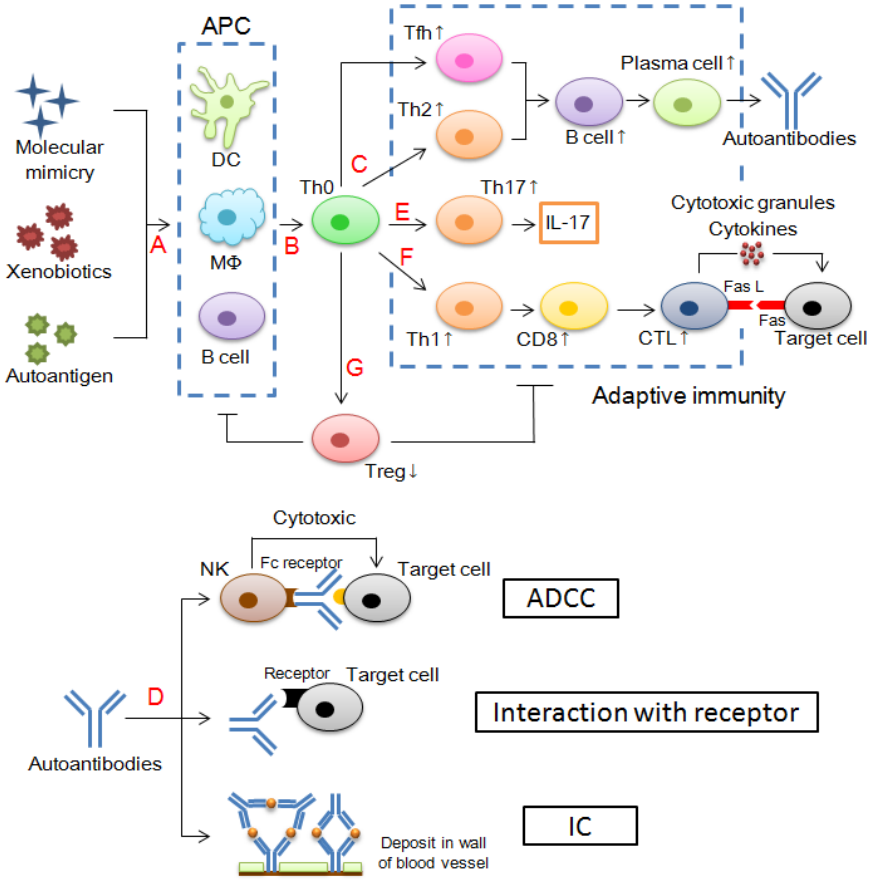

Fig. 1 Autoimmunity is a result of a multi-orchestrated immune response [7, *modified*]. **A** The recognition of molecular mimicry, xenobiotics and autoantigen by APC such as DC, MΦ, and NK lead to initiation of autoimmunity. **B** The activated APC present antigenic peptides to Th0 lymphocytes, which then differentiate into Th2, Tfh, Th17, Th1 or Treg. **C** B cells are activated by Tfh and Th2, and then become mature and differentiate into plasma cells. **D** Through antibody-dependent cell-mediated cytotoxicity (ADCC), interaction with receptor of target cells and deposition of immune complex (IC), and autoantibodies can mediate autoimmune diseases.

Chapter 1: Intravenous immunoglobulin (IVIg) acts directly on steady-state B cells to suppress their homeostatic expansion

1.1. Introduction

B cells are a type of lymphocytes, and their role in immune system is secreting antibodies to eliminate pathogenetic antigens such as virus and bacteria. However, B cells also play a critical role in the pathogenic inflammatory response by producing autoantibodies in autoimmune disorders [7]. For example, the level of anti-nuclear antibodies to double-stranded DNA, Sjogren's syndrome (SS)-A and SS-B in plasma are diagnostic criteria for systemic lupus erythematosus (SLE) and SS [8,9]. IVIg has been evaluated for its therapeutic effects in above-mentioned autoimmune diseases characterized by over production of autoantibodies.

Previous studies have proposed several inhibitory activities of IVIg on B cells. IVIg suppresses B cell activation through agonistic binding to inhibitory receptors CD22 [24,25] and FcγRIIB [26] on B cells. IVIg also interacts with B cell receptor (BCR) [27,28] or toll-like receptors (TLR) [29,30] to negatively regulate B cell

activation. Although those B cell immunosuppressive activities of IVIg acts on activated B cells, the impact of IVIg on steady-state B cells still remains to be elucidated.

Dysregulation of immune homeostasis can lead to induction of autoimmune diseases [31]. Especially, failure of B cell homeostasis in steady-state mediates autoimmune disorders, and hyper-activation of B cells is involved in the deterioration of chronic inflammation [32,33]. Thus, keeping B cells in normal homeostasis is important to prevent chronic inflammation leading to autoimmune diseases, and to test whether IVIg affects B cell homeostatic expansion is intriguing trial for elucidation of B cell inhibitory activity of IVIg.

In this chapter, I show that IVIg acts directly on steady-state B cells, and suppresses their homeostatic expansion accompanied with B cell-specific cell aggregation. Present results provide new insight into the B cell regulatory activities of IVIg.

1.2. Materials and methods

1.2.1. Mice and ethical statement

Five-week-old female BALB/c mice were purchased from Charles River Laboratories Japan (Kanagawa, Japan) and kept under specific pathogen-free conditions until use. All animal experiments were followed the protocols approved by the Committee on Animal Experimentation of Hiroshima University, Japan.

1.2.2. Reagents

Pooled human immunoglobulin agent (Sanglopor® I.V. Infusion) and human albumin were purchased from CSL Behring and FUJIFILM Wako Pure Chemical Corporation (Osaka, Japan) respectively. Purchased agent and albumin were reconstituted with endotoxin-free saline (Otsuka Pharmaceutical Factory, Tokushima, Japan) as 200 mg/ml aliquots and kept at -20˚C until use. All chemicals were biochemical grade or cell culture grade.

1.2.3. Purification or depletion of B and T cells from murine splenocytes

CD19-positive ($CD19^+$) B cells or CD3-positive ($CD3^+$) T cells were purified from splenocytes of BALB/c mice by using anti-CD19 antibody-conjugated magnetic beads or Pan T cell Isolation Kit II (Miltenyi Biotec, Bergisch-Gladbach, Germany) following the manufacturer's instruction. For depletion of $CD19^+$ B cells or $CD3^+$ T cells, splenocytes were also treated anti-CD19 antibody-conjugated magnetic beads or Pan T cell Isolation Kit II following the manufacturer's instruction.

1.2.4. Cell labeling with fluorescent dye

3×10^6 purified $CD19^+$ B cells were stained with 400-fold-diluted Orange Fluorescent Cytoplasmic Membrane Staining Kit (Takara Bio, Shiga, Japan) for 2 min. 5×10^6 purified $CD3^+$ T cells were stained with 1 μM 5-(and 6)-carboxyfluorescein diacetate succinimidyl ester (CFSE; Affymetrix Japan, Tokyo, Japan) for 10 min. Labeled B cells, T cells and non-labeled non-B/T cells were reconstituted for original subset rate of splenocytes.

1.2.5. Cell culture

For proliferation assay, 3×10^5 whole splenocytes, B or T cell-depleted splenocytes, and purified B or T cells were cultured with 10 mg/ml IVIg or human albumin, 50 μg/ml mitomycin C, or saline as a vehicle control in 200 μl of RPMI medium (Sigma-Aldrich, St. Louis, MO, USA), containing 10% fetal bovine serum (FBS; Sigma-Aldrich), 50 μM 2-mercaptoethanol (Nacalai Tesque, Kyoto, Japan), 100 units/ml penicillin (Thermo Fisher Scientific, Waltham, MA, USA) and 100 μg/ml streptomycin (Thermo Fisher Scientific), for 48 h in 96-well flat-bottom culture plates (Corning, Corning, NY, USA).

For microscopic analysis, 3×10^5 naive splenocytes, B or T cell-depleted splenocytes, purified B or T cells, or B and T cell-labeled splenocytes were cultured with 10 mg/ml IVIg or human albumin, 50 μg/ml mitomycin C, or saline in 200 μl of RPMI medium for 48 h in triple-well glass-base dish (Asahi Glass, Tokyo).

1.2.6. Proliferation assay

Cell proliferation was estimated by BrdU incorporation during the last 18 h of 48-hour cultivation. BrdU incorporation was determined by Cell Proliferation Enzyme-linked Immunosorbent Assay (ELISA) BrdU (colorimetric) Kit (Roche

Diagnostics, Mannheim, Germany) following the manufacturer's instruction.

1.2.7. Microscopic analysis

Fluorescent dye-labeled splenocytes were detected by fluorescence microscopy (BZ-9000, Keyence, Osaka, Japan) after 48 h cultivation.

1.2.8. Neutralization of Fcγ receptors (CD16/32) and integrin β2 (CD18)

Naive splenocytes were incubated with 16 μg/ml anti-CD16/32 antibody (eBioscience™, Thermo Fisher Scientific), 16 μg/ml rat IgG2a isotype control antibody (eBioscience™, Thermo Fisher Scientific), 20 μg/ml anti-CD18 antibody (BioLegend, San Diego, CA, USA), or 20 μg/ml rat IgG2a isotype control antibody (BioLegend) for 15 min at 4˚C. Then, 20 mg/ml IVIg or albumin, 100 μg/ml mitomycin C or saline was added, and splenocytes were cultured for 48 h. The final concentration of each reagent was 8 μg/ml anti-CD16/32 antibody or their isotype control antibody, 10 μg/ml anti-CD18 antibody or their isotype control antibody, 10 mg/ml IVIg and albumin, and 50 μg/ml mitomycin C.

1.2.9. Statistical analysis

Data are represented as mean ± SD. Representative data are from three independent experiments. A non-repeated analysis of variance (ANOVA) was applied to the comparisons of data among four groups; when a difference was significant, a post hoc analysis using the Turkey's test was performed. Statistical significance was defined as $p < 0.05$.

1.3. Results

1.3.1. IVIg suppresses proliferation of murine splenocytes in steady-state

To test the immunosuppressive capacity of IVIg, I first cultured naive murine splenocytes with IVIg and assessed its anti-proliferative effect. IVIg suppressed proliferation of unstimulated splenocytes as compared with these stimulated with human albumin and saline (Fig. 2A). In addition, I also found that IVIg induced of cell aggregation (shown as arrows in Fig. 2B). These results show that IVIg fulfills two effects on steady-state immune cells; IVIg suppressed homeostatic proliferation of splenocytes accompanied with cell aggregation.

1.3.2. IVIg suppresses homeostatic proliferation of B cells

To explore the responsible cell types of IVIg-derived immunosuppressive activity in steady-state, I depleted or isolated major immune cells, B cell and T cells, from whole splenocytes, and tested the immunosuppressive activity of IVIg on these fractionated cell subsets. IVIg significantly suppressed homeostatic proliferation of whole splenocytes ("Whole splenocytes" in Fig. 3). However, B cell-depletion from splenocytes abolished homeostatic proliferation seen on whole splenocytes ("B

cell-depleted" in Fig. 3). In contrast, T cell-depletion from splenocytes was not affected on induction of homeostatic proliferation, and IVIg suppressed the homeostatic expansion of T cell-depleted splenocytes ("T cell-depleted" in Fig. 3). Furthermore, IVIg significantly suppressed homeostatic proliferation of purified B cells ("Purified B cells" in Fig. 3), and purified T cells did not possess homeostatic proliferation ("Purified T cells" in Fig. 3). These *in vitro* data suggest that steady-state B cells show the activity of homeostatic expansion, and IVIg suppresses their homeostatic proliferation.

1.3.3. IVIg induces B cell-specific aggregation

The B cell immunosuppression by IVIg treatment was accompanied by cell aggregation (Fig. 2B). To investigate the responsible cell population of IVIg-mediated cell aggregation, I also depleted or isolated B cells and T cells from splenocytes. IVIg induced cell aggregation in whole splenocytes culture ("Whole splenocytes" in Fig. 4A). T cell-depletion from splenocytes had no effect on IVIg-driven cell aggregation seen on whole splenocytes ("T cell-depleted" in Fig. 4A), but B cell-depletion from splenocytes abolished induction of cell aggregation ("B cell-depleted" in Fig. 4A). Moreover, IVIg induced cell aggregation on purified B cells ("Purified B cells" in Fig. 4A), and purified T cells failed to form cell aggregation upon stimulation with IVIg ("Purified T cells" in

Fig. 4A). Then, I stained B cells and T cells with fluorescent dyes to confirm whether the IVIg-triggered cell aggregation consisted of only B cells. IVIg induced aggregation of orange dye-labeled B cells, but not green dye-labeled T cells ("IVIg" in Fig. 4B). These data suggest that B cells are essential for IVIg-driven cell aggregation, and the cell aggregates mainly composed of B cells.

1.3.4. Fcγ receptors and integrin β2 are not involved in IVIg-mediated aggregation and suppression of homeostatic proliferation

Above results suggest that IVIg directly acts on steady-state B cells to suppress their homeostatic expansion. Previous study reported that IVIg induced CD32 (a low-affinity Fcγ receptor; FcγRII) -mediated platelet aggregation [34]. CD32 is also expressed on the surface of B cells. Furthermore, Fcγ receptors are proposed as the key target molecules of immunosuppressive function of IVIg [35,36]. To analyze involvement of Fcγ receptors in IVIg-drived B cell aggregation, I tested whether neutralizing antibody against Fcγ receptors (CD16 and CD32) canceled induction of B cell aggregation. Treatment with anti-CD16/CD32 antibody was not affected on induction of B cell aggregation, shown as orange clusters (Fig. 5A). In addition, B cells express adhesion molecule CD18 (integrin β2), which is important molecule for B

cell aggregation [37]. I also tested the involvement of CD18 in IVIg-derived B cell aggregation by using neutralizing antibody against CD18. B cell aggregation, shown as orange cluster, was still intact even when co-cultured with anti-CD18 antibody (Fig. 5B). These data indicate that Fcγ receptors and integrin β2 are unnecessary for B cell aggregation induced by IVIg.

To confirm whether Fcγ receptors and integrin β2 were needed for inhibition of B cell homeostatic proliferation by IVIg treatment, I also assessed immunosuppressive activity of IVIg upon co-culture with neutralizing antibody against CD16/CD32 or CD18. IVIg significantly suppressed homeostatic proliferation of splenocytes co-cultured with anti-CD16/CD32 as well as with anti-CD18 (Fig. 6). These results suggest that Fcγ receptors and CD18 are also dispensable for suppression of B cell homeostatic proliferation by IVIg treatment.

1.4. Discussion

In this chapter, I revealed that IVIg acted directly on steady-state B cells and suppressed their homeostatic proliferation. The B cell inhibitory activity was accompanied with B cell aggregation, and adhesion molecule (integrin β2/CD18) and FcγRs (CD16/32) on B cells were dispensable for IVIg-driven B cell regulation. These results provide a new insight into immunosuppressive capacity of IVIg on dysregulation of B cell homeostasis leading to abnormal B cell activation.

An intriguing point on the homeostatic expansion of B cells is that the other lymphocytes do not possess such homeostatic proliferation like B cells. Indeed, B cell-depletion from splenocytes abolished homeostatic proliferation seen on whole splenocytes ("B cell-depleted" in Fig. 3), and purified T cells did not growth in steady-state ("Purified T cells" in Fig. 3). These findings suggest that B cell-specific growth factors regulate B cell homeostatic proliferation, and IVIg suppresses their activity triggered by those growth factors. B cell activating factor (BAFF) is known as a modulator of B cell homeostasis [38]. The serum level of BAFF is elevated in patients with SLE and positively correlates with disease activity [39,40]. Besides, the level of BAFF correlates with the titer of autoantibodies in SS [41]. A plausible

inhibitory mechanism of IVIg would be that IVIg suppresses BAFF-mediated B cell homeostatic proliferation through inhibition of BAFF reseptor (BAFFR, TNF-receptor super-family) signaling. B cells express BAFFR on its cell surface and the receptor triggers the non-canonical NF-κB-dependent pathway [42,43]. In addition, binding of BAFF to BAFFR activates the phosphoinositide-3-kinase (PI3K)-dependent signaling cascade [44]. To test whether IVIg acts on BAFF receptor and suppresses these signaling pathways would be intriguing future issue. Furthermore, previous reports suggest that activation of B cells is contributed by sex hormones [45], which play essential roles in sexual development of female. Actually, SLE characterized by the production of multiple autoantibodies is higher prevalence in women than men [46]. For concrete example, it has been demonstrated that treatment of women with estrogen (one of the sex hormone) or exposure of human peripheral blood mononuclear cells (PBMC) to estrogen lead to higher levels of immunoglobulins [47]. Another sex hormone, prolactin, enhances secretion of BAFF and immunoglobulins [48]. Prolactin is produced by B cells, and B cells also express prolactin receptors [49]. Thus, these sex hormones would be the responsible growth factor for homeostatic expansion of B cells. Most of estrogen's effects are mediated two specific intracellular receptors, estrogen receptor (ER) α and β, which function as ligand- activated nuclear

transcription factors producing genomic effects [50]. The JAK/STAT pathway is the main signaling pathway used by prolactin receptors [51,52]. To assess participation of these molecules and pathways to homeostatic expansion of B cells would provide insights into identification of the B cell regulatory mechanism by IVIg.

Another unsolved issue is identification of target molecule to suppress B cell homeostatic proliferation and to form B cell aggregation by IVIg. In this thesis, I showed that neutralization of plausible molecules (integrin β2 and FcγRs) failed to abrogate anti-proliferative activity and formation of aggregation by IVIg (Fig. 5 and 6). In a preliminary trial based on the hypothesis that IVIg acted on a B cell surface target molecule and fulfilled its inhibitory activity, I found that immunoprecipitates of B cell lysate by IVIg contained myosin-9 (data not shown). This molecule is involved in infection of Epstein-Barr virus (EBV) on nasopharyngeal epithelial cell membrane [53]. EBV also infects B cells to cause lymphomas [53]. Myosin-9 would be a candidate of the target of IVIg, and further analysis is required for decision of responsible antigen that binds to IVIg.

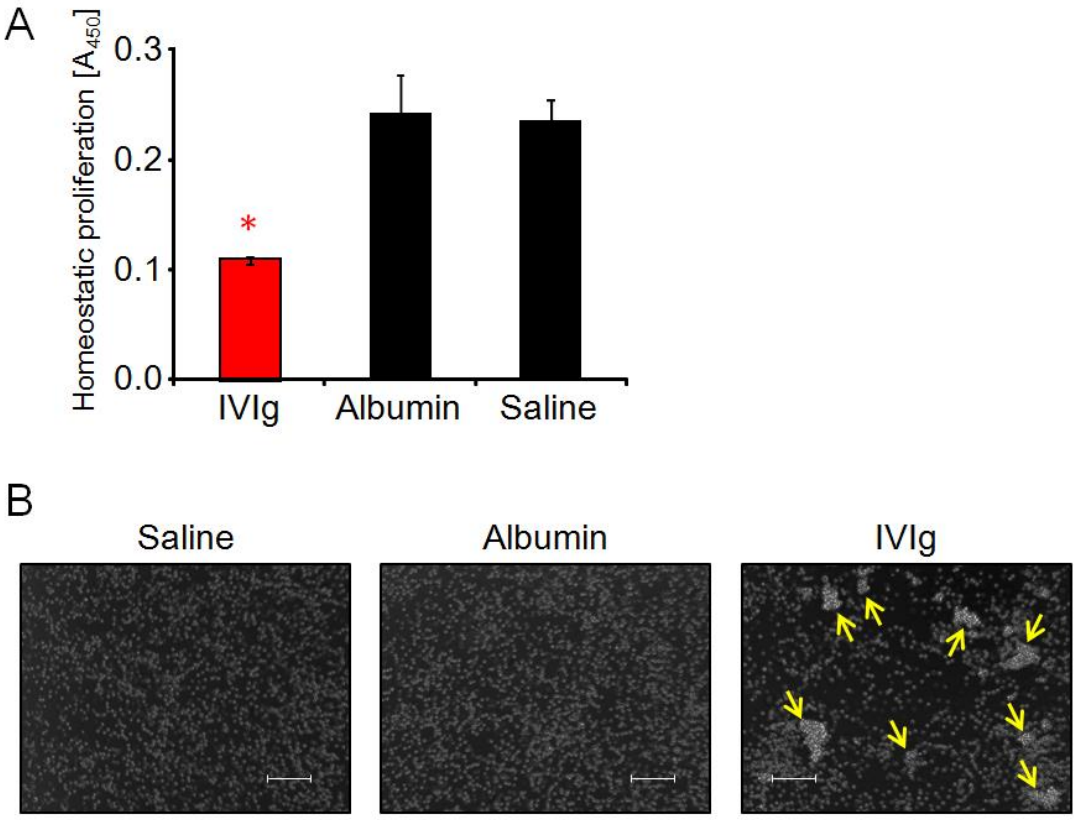

Fig. 2 IVIg suppresses proliferation of murine splenocytes in steady-state. **A** IVIg suppressed homeostatic proliferation of murine splenocytes. Unstimulated murine splenocytes were cultured with IVIg (10 mg/ml), albumin (10 mg/ml) or saline for 48h. Proliferation was estimated by BrdU incorporation. *Significantly different at $p < 0.05$ among saline, albumin, and IVIg by non-repeated ANOVA and the post hoc Tukey test. Data are presented as means ± SD (n = 3). **B** IVIg induced cell aggregation. Each image is shown cultured splenocytes with IVIg (10 mg/ml), albumin (10 mg/ml) or saline for 48 h, respectively. All scale bars represent 100 μm.

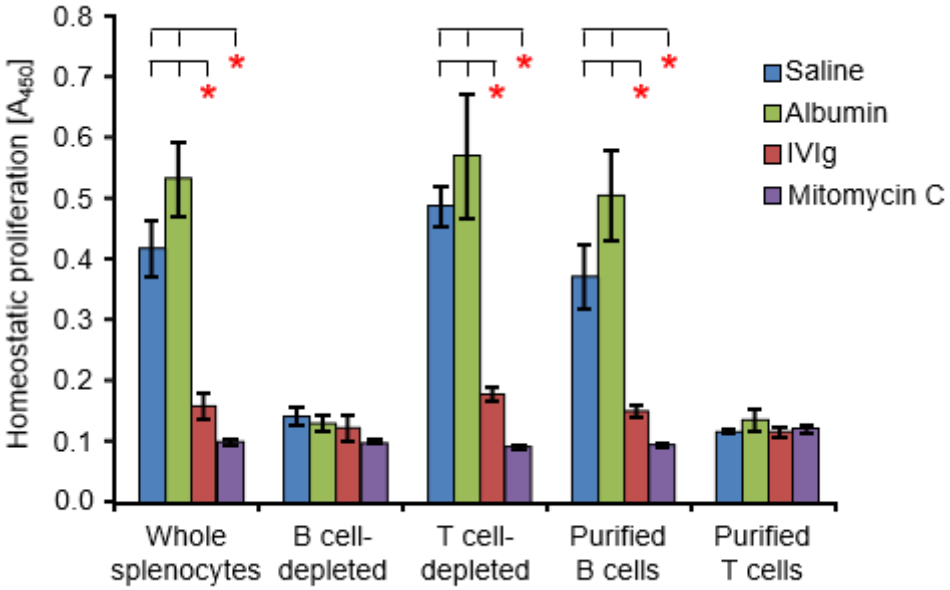

Fig. 3 IVIg suppresses homeostatic proliferation of B cells. Whole splenocytes, B cell-depleted splenocytes, T cell-depleted splenocytes, purified B cells or purified T cells were cultured with IVIg (10 mg/ml), albumin (10 mg/ml), mitomycin C (50 μg/ml) or saline. The proliferation was measured by BrdU incorporation. *Significantly different at $p < 0.05$ among saline, albumin, IVIg, and mitomycin C by non-repeated ANOVA and the post hoc Tukey test. Data are presented as means ± SD (n = 3).

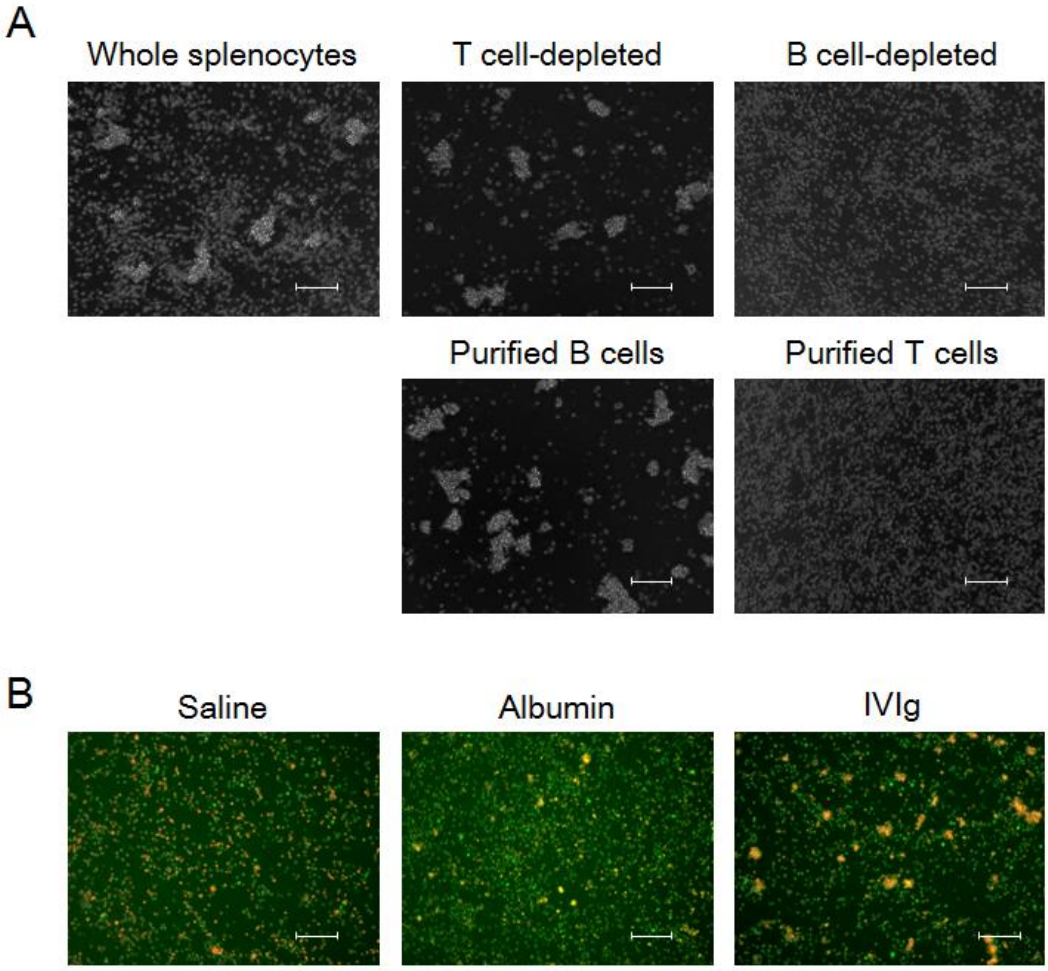

Fig. 4 IVIg induces B cell-specific aggregation. **A** IVIg induced B cell aggregation. Whole splenocytes, T cell-depleted splenocytes, B cell-depleted splenocytes, purified B cells or purified T cells were cultured with IVIg (10 mg/ml) for 48 h. All scale bars represent 100 μm. **B** IVIg induced B cell aggregation in reconstituted splenocytes. B cells or T cells were stained with orange or green fluorescent dye, respectively. Orange dye-labeled B cells, green dye-labeled T cells and unstained non-B/T cells were reconstituted to consist of B and T cell-labeled splenocytes. Reconstituted splenocytes were cultured with IVIg (10 mg/ml), albumin (10 mg/ml) or saline for 48 h and analyzed by a fluorescence microscopy. All scale bars represent 100 μm.

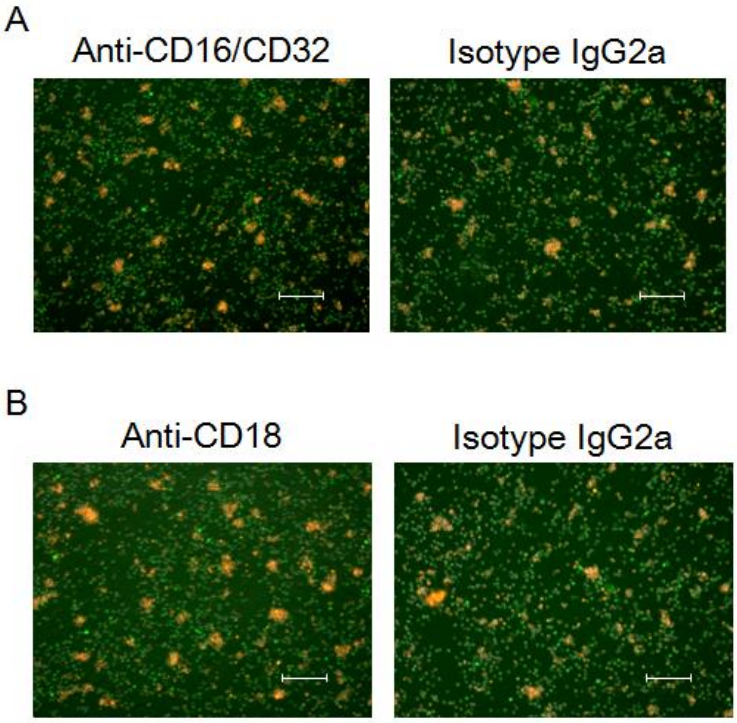

Fig. 5 Fcγ receptors and integrin β2 are not involved in IVIg-mediated cell aggregation. **A** CD16 and CD32 were dispensable for IVIg-drived cell aggregation. Splenocytes pre-incubated with anti-CD16/CD32 or isotype IgG2a antibody were cultured with IVIg (10 mg/ml) for 48 h and analyzed by a fluorescence microscopy. All scale bars represent 100 μm. **B** CD18 was dispensable for IVIg-derived cell aggregation. Splenocytes pre-incubated with anti-CD18 or isotype IgG2a antibody were cultured with IVIg (10 mg/ml) for 48 h and analyzed by a fluorescence microscopy. All scale bars represent 100 μm.

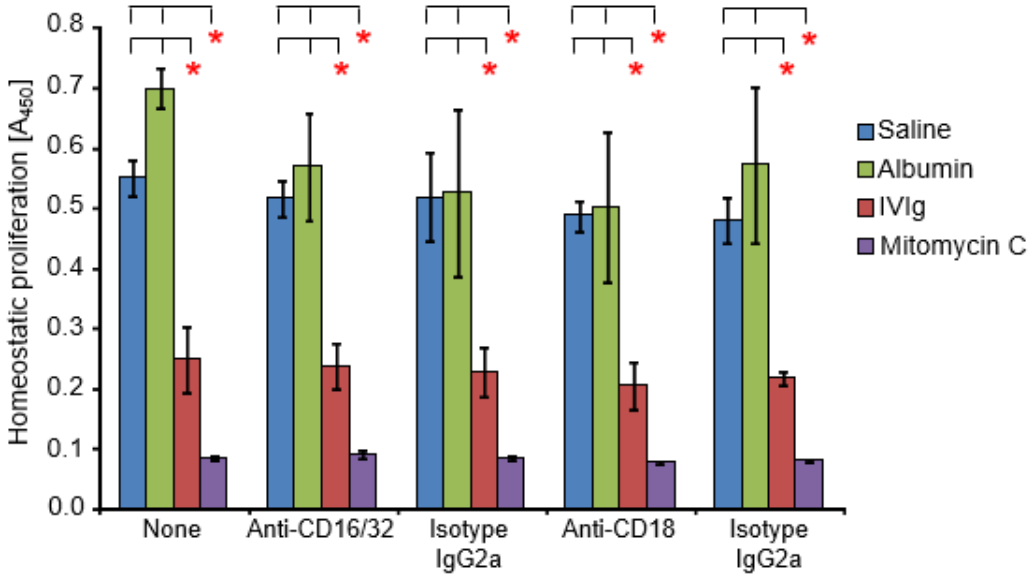

Fig. 6 Fcγ receptors and integrin β2 are not involved in IVIg-driven suppression of homeostatic proliferation. Fcγ receptors and integrin β2 were unnecessary for IVIg-drived suppression of homeostatic proliferation. Splenocytes pre-incubated with anti-CD16/CD32, anti-CD18 or isotype IgG2a antibody were cultured with IVIg (10 mg/ml), albumin (10 mg/ml), mitomycin C (50 μg/ml) or saline. The proliferation was measured by BrdU incorporation. *Significantly different at $p < 0.05$ among saline, albumin, IVIg, and mitomycin C by non-repeated ANOVA and the post hoc Tukey test. Data are presented as means ± SD (n = 3).

Chapter 2: IVIg acts directly on conventional T cells to suppress their activation upon T cell receptor (TCR) ligation

2.1. Introduction

In the previous chapter, I found that IVIg acts directly on steady-state B cells, and suppresses their homeostatic proliferation accompanied with B cell aggregation. However, not only B cells but also T cells cause autoimmune diseases. In fact, T cell-driven pathogenesis is observed in several autoimmune disorders. For example, high level of IL-17 produced by Th17 cells progresses inflammation in patients of rheumatoid arthritis (RA) [11] and multiple sclerosis (MS) [14], and cytotoxic T cells provoke type 1 diabetes (T1D) [15] and primary biliary cirrhosis (PBC) [16]. Besides, decreased Treg which negatively regulates immune responses leads to deficiency of immune tolerance in patients with SLE, MS, and RA [17,18,19]. IVIg has therapeutic effects on those T cell-triggered autoimmune diseases.

Recent works have proposed T cell regulatory mechanisms of IVIg, but most of them suggest that IVIg expands Treg to suppress T cell activation. IVIg induces Treg expansion through the antigen presentation of IgG Treg epitopes (Tregitopes, IVIg

Fc-derived antigen peptides) [54]. IL-33 [55] or prostaglandin E2 [56] produced by IVIg-treated antigen presenting cells (APC) also expands Treg. Therefore, all of those T cell immunosuppressive actions of IVIg are indirectly fulfilled *via* APC and Treg, but the direct impact of IVIg on T cells remains to be elucidated.

In this chapter, I show that IVIg acts directly on conventional T cells and suppresses their activation upon TCR ligation. Present results provide new mechanistic insight into the T cell regulatory activity of IVIg.

2.2. Materials and methods

2.2.1. Mice and ethical statement

Five-week-old female BALB/c mice were purchased from Charles River Laboratories Japan (Kanagawa, Japan) and kept under specific pathogen-free conditions until use. All animal experiments were followed the protocols approved by the Committee on Animal Experimentation of Hiroshima University, Japan.

2.2.2. Reagents

Pooled human immunoglobulin agent (Sanglopor® I.V. Infusion) and human albumin was purchased from CSL Behring and FUJIFILM Wako Pure Chemical Corporation (Osaka, Japan) respectively. Purchased agent and albumin were reconstituted with endotoxin-free saline (Otsuka Pharmaceutical Factory) as 200 mg/ml aliquots and kept at -20˚C until use. Phytohemagglutinin (PHA), concanavalin A (Con A) and lipopolysaccharide (LPS) were purchased from Sigma-Aldrich. PHA and LPS were reconstituted with phosphate buffered saline (PBS; FUJIFILM Wako Pure Chemical Corporation) as 1 mg/ml aliquots, and Con A was reconstituted with dimethyl sulfoxide (DMSO; Sigma-Aldrich) as 5 mg/ml aliquots. All stimulants aliquots kept at

-20˚C until use. All of the chemicals used were of biochemical grade or cell culture grade.

2.2.3. Cultivation of splenocytes with immunostimulants

3×10^5 splenocytes prepared from female BALB/c mice were cultured with 1.25, 2.5, 5, 10, or 20 μg/ml PHA, 0.125, 0.25, 0.5, or 1 μg/ml Con A, 0.125, 0.25 0.5, 1, 2, or 4 μg/ml LPS, or 0.125, 0.25 0.5, 1 μg/ml immobilized anti-CD3 antibody upon co-stimulation with 10 mg/ml IVIg or human albumin in 200 μl of culture medium. The culture medium based on RPMI medium (Sigma-Aldrich), and supplemented 10% fetal bovine serum (FBS; Sigma-Aldrich), 50 μM 2-mercaptoethanol (Nacalai Tesque) 100 units/ml penicillin (Thermo Fisher Scientific) and 100 μg/ml streptomycin (Thermo Fisher Scientific) for 48 h in 96-well flat-bottom culture plates (Corning). The cell proliferation was estimated by BrdU incorporation during the last 18 h of the 48-h culture. Cell Proliferation Enzyme-linked Immunosorbent Assay (ELISA) BrdU (colorimetric) Kit (Roche Diagnostics) was used for measurement of BrdU incorporation following the manufacturer's instructions.

2.2.4. Flow cytometoric analysis of cell cycle arrest and apoptosis

6×10^5 splenocytes were cultured with 60 μg/ml PHA co-cultured with 30 mg/ml IVIg or human albumin for 48 h. The cultured splenocytes were stained with allophycocyanin (APC)-labeled anti-CD3 antibody (eBioscince, Thermo Fisher Scientific), and co-stained with BrdU Flow Kit (BD Pharmingen, BD Biosciences) or fluorescein isothiocyanate (FITC)-conjugated Annexin V (BioLegend, San Diego, CA, USA) following manufacturer's instruction. The labeled splenocytes were analyzed by flow cytomerter gating on $CD3^+$ T cells to estimate cell cycle distribution or fluorescent intensity of Annexin V. FlowJo software (FlowJo, Ashland, OR, USA) was used for analysis of flow cytometoric data.

2.2.5. Purification of T cells from murine splenocytes

$CD3^+$ T cells were purified by using Pan T cell Isolation Kit II (Miltenyi Biotec), and $CD25^-$ T cells were isolated from purified $CD3^+$ T cells by using CD25 MicroBead Kit (Miltenyi Biotec). Both kits were used following the manufacturer's instructions.

2.2.6. T cell culture with phytohemagglutinin (PHA) or anti-CD3 antibody

3×10^5 of purified $CD3^+$ T cells or $CD25^-$ T cells were cultured with 1.25, 2.5, 5, 10, or 20 μg/ml PHA, or 0.125, 0.25 0.5, 1 μg/ml immobilized anti-CD3 antibody upon co-stimulation with 10 mg/ml IVIg or human albumin in 200 μl of culture medium. The cell proliferation was estimated by BrdU incorporation during the last 18 h of the 48-h culture. Cell Proliferation Enzyme-linked Immunosorbent Assay (ELISA) BrdU (colorimetric) Kit (Roche Diagnostics) was used for measurement of BrdU incorporation following the manufacturer's instructions.

2.2.7. Flow cytometoric analysis of regulatory T cells (Treg)

1.2×10^6 of purified $CD3^+$ T cells or $CD25^-$ T cells were cultured with 1 μg/ml immobilized anti-CD3 antibody upon co-stimulation with 10 mg/ml IVIg or human albumin in 200 μl of culture medium. After cultivation, the cells were stained with APC-labeled anti-CD3 antibody (eBioscince, Thermo Fisher Scientific), and treated by Foxp3/Transcription Factor Stain Buffer (eBioscince, Thermo Fisher Scientific) to co-stain with phycoerythrin (PE)-conjugated anti-Foxp3 antibody (eBioscince, Thermo Fisher Scientific). The stained cells were analyzed by a flow cytomerter.

FlowJo software was used for analysis of flow cytometoric data.

2.2.8. Analysis of cytokine production

Production of interleukin (IL)-10 and IL-2 in supernatant of above T cell culture was estimated by using IL-10 Mouse Uncoated ELISA Kit (Thermo Fisher Scientific) or sandwich enzyme-linked immunosorbent assay using ELISA MAX^{TM} Standard Set Mouse IL-2 (BioLegend). These kits were used following the manufacturer's instructions.

2.2.9. IL-2 supplementation assay

250 pg/ml recombinant IL-2 (BioLegend) was added to above T cell culture stimulated with 1 μg/ml anti-CD3 antibody and co-stimulated with 10 mg/ml IVIg for 48 h. After cultivation, the proliferations were estimated by proliferation assay. The T cell proliferation was estimated by BrdU incorporation during the last 18 h of the 48-h culture. Cell Proliferation Enzyme-linked Immunosorbent Assay (ELISA) BrdU (colorimetric) Kit (Roche Diagnostics) was used for measurement of BrdU incorporation following the manufacturer's instructions.

2.2.10. Western blotting

1×10^7 $CD3^+$ T cells were cultured with 1 μg/ml immobilized anti-CD3 antibody (BioLegend) supplemented with or without 10 mg/ml IVIg for 0, 0.5, 1, 3, 6 h. The cultured T cells were washed with chilled PBS twice, and lysed with a lysis buffer [50 mMTris-HCl/ 150 mM NaCl/ 1% Triton-X100/ 0.1% Sodium dodecyl sulfate (SDS), pH 7.5] supplemented with Complete Protease Inhibitor Cocktail (Roche Diagnostics), Aprotinin (Roche Diagnostics), Pefabloc SC (Roche Diagnostics), and Phosphatase Inhibitor Cocktail (Nacalai tesque, Kyoto, Japan) on ice for 30 min. For the separation of nuclear and cytoplasmic proteins, cultured T cells were treated with NE-PER™ Nuclear and Cytoplasmic Extraction Reagents (Thermo Fisher Scientific) supplemented with Complete Protease Inhibitor Cocktail (Roche Diagnostics), Aprotinin (Roche Diagnostics), Pefabloc SC (Roche Diagnostics). Whole cell lysates or separated nuclear proteins were separated by sodium dodecyl sulfate polyacrylamide gel electrophoresis (SDS-PAGE) under reducing conditions. Separated proteins were transferred onto a PVDF membrane (Merck Millipore LTd., Sigma-Aldrich). The membrane was incubated with anti-IκB, GAPDH, NFAT1, Lamin A/C, phospho-Erk1/2, Erk, phospho-ZAP-70 or ZAP-70 antibody respectively at 4˚C overnight and then horseradish peroxidase (HRP)-conjugated anti-rabbit IgG secondary antibody at 1h

room temperature. Detection of positive signals was performed by ECL Prime Western Blotting Detection System (GE Healthcare Bio-Sciences, Tokyo, Japan).

2.2.11. Immunoprecipitation

Purified T cells were cultured with immobilized anti-CD3 antibody (1 μg/ml) supplemented with or without IVIg (10 mg/ml) for 0, 3, or 6 h. After cultivation, T cells were harvested and washed twice with ice cold PBS. Whole protein was extracted from the cultured cells using a lysis buffer [50 mMTris-HCl/ 150 mM NaCl/ 1% Triton-X100/ 0.1% SDS, pH 7.5] supplemented with complete protease inhibitor cocktail (Roche Diagnostics), aprotinin (Roche Diagnostics), Pefabloc SC (Roche Diagnostics), and phosphatase inhibitor cocktail (Nacalai Tesque) on ice for 30 min. Tyrosine-phosphorylated proteins were immunoprecipitated using agarose-conjugated anti-phosphotyrosine antibody (Merck Millipore, Sigma-Aldrich)

2.2.12. nano LC-MS/MS analysis

Fractionated protein bands in a SDS-PAGE gel (visualized by coomassie brilliant blue staining) were excised and digested using sequencing grade modified trypsin (Promega Corporation, WI). Resultant peptide mixtures were analyzed by nano

LC-MS/MS using an Ultimate 3000 RSLCnano (Thermo Fisher Scientific) coupled to a LTQ Orbitrap XL (Thermo Fisher Scientific). Identification of proteins was performed with Proteome Discoverer v2.2 (Thermo Fisher Scientific) and Mascot (Matrix Science Ltd, London, UK).

2.2.13. Statistical analysis

Data are represented as means ± SD. Representative data are from three independent experiments. A non-repeated analysis of variance (ANOVA) was applied to the comparisons of data among four groups; when a difference was significant, a post hoc analysis using the Turkey test was performed. Statistical significance was defined as $p < 0.05$.

2.3. Results

2.3.1. IVIg suppresses proliferation of splenocytes upon stimulation with T cell-tropic stimulants

To test T cell immunosuppressive capacity of IVIg, splemocytes stimulated with T cell-tropic stimulants (PHA and ConA) were cultured with IVIg. IVIg suppressed proliferation of splenocytes stimulated with PHA or Con A (Fig. 7A and B), but not that stimulated with an activator of innate immunity (LPS, Fig. 7C). These results suggest that IVIg preferentially suppress T cell activation.

2.3.2. IVIg induces G_1 cell cycle arrest of T cells, but does not induce apoptosis

To confirm whether IVIg induces G_1 cell cycle arrest and/or apoptosis of T cells, I analyzed cell cycle distribution of splenocytes stimulated with PHA by flow cytometric analysis gated on $CD3^+$ T cells. IVIg co-stimulation increased percentage of $CD3^+$ T cells in G_1 phase (53.4% ± 1.53, Fig. 8A right and 8B) as compared with albumin (30.5% ± 1.37) and saline (32.6 ± 2.76). By contrast, T cells in S phase were decreased by IVIg treatment (7.6% ± 1.30) as compared with albumin (35.5% ± 0.36) and saline (31.5% ± 1.21). These results show that IVIg induces G_1 cell cycle arrest of

T cells. On the other hand, intensity of annexin V was comparable with T cells treated with IVIg, albumin and saline (Fig. 8C), showing that IVIg does not induce apoptosis of T cells.

2.3.3. IVIg suppresses proliferation of purified T cells upon TCR ligation

To assess whether IVIg directly suppress T cell activation, I estimated immunosuppressive capacity of IVIg on purified T cells. IVIg suppressed proliferation of purified T cells (Fig. 9B) upon stimulation with PHA, similar to the same manner seen in whole splenocytes (Fig. 9A). I also assessed whether IVIg can suppress proliferation of T cells stimulated with anti-CD3 antibody (closer to physiological stimulation). IVIg suppressed proliferation of splenocytes (Fig. 9D) and purified T cells (Fig. 9E) stimulated with anti-CD3 antibody. These results indicate that IVIg acts directly on T cells and suppresses their activation upon TCR ligation.

I next tested whether naturally-occurring Treg (nTreg) was involved in the above T cell regulatory activity. The immunosuppressive activity of IVIg on T cells was still intact after depletion of $CD25^+$ T cells (nTreg population) from purified T cells (Fig. 9C and F). These results suggest that IVIg directly acts on non-Treg conventional T cells to suppress their activation.

2.3.4. IVIg does not induce expansion of $CD4^+$ $Foxp3^+$ Treg

Treg is classified into nTreg that develops in the thymus or inducible Treg (iTreg) that differentiate in the periphery. In the previous section, I revealed that the T cell regulatory activity of IVIg was still intact in the absence of $CD25^+$ nTreg (Fig. 9C and F), but the possibility still remained that IVIg co-stimulation could induce expansion of iTreg. To test whether IVIg triggers expansion of iTreg, IVIg-treated purified T cells and $CD25^-$ T cells were analyzed by flow cytometoric analysis. IVIg failed to expand $CD4^+$ $Foxp3^+$ Treg in purified T cells (Fig. 10A) as well as in $CD25^-$ T cells (Fig. 10B). Furthermore, I quantified production of IL-10, which behaves inhibitory cytokine and produced by $Foxp3^-$ Treg (Tr1 cells). IVIg did not induce IL-10 production (Fig. 10D), suggesting that Tr1 cells were not inducted by IVIg treatment. Taken together, these results show that IVIg does not have any impact on expansion of Treg as well as on production of IL-10.

2.3.5. IVIg negatively regulates TCR signaling

The fact that IVIg suppressed proliferation of purified T cells stimulated with anti-CD3 antibody (Fig. 9E and F) without expansion of Treg (Fig. 10) suggests that IVIg can directly suppress TCR signaling. To obtain stronger evidence that IVIg

suppress TCR signaling, I quantified IL-2 production induced by activation of TCR signaling. IVIg co-stimulation inhibited IL-2 production from purified T cells upon stimulation with anti-CD3 antibody (Fig. 11A). Furthermore, adding back of recombinant IL-2 to IVIg-treated T cells abrogated IVIg-driven regulatory activity of T cell proliferation (Fig. 11B). These results indicate that IVIg perform its T cell regulatory activity by inhibition of TCR signaling.

Next, I tested whether IVIg actually inhibited TCR signaling. TCR signaling branches out along three major pathways [the nuclear factor-κB (NF-κB), Ca^{2+}-calcineurin-nuclear factor of activated T cells (NFAT), and mitogen-activated protein kinase (MAPK)-AP1 pathways], all of which are essential for full activation of T cells [57]. IVIg co-stimulation impaired degradation of IκB, which inactivated NF-κB transcription factor (Fig. 12A). I also found that IVIg inhibited nuclear translocation of NFAT1 transcription factor (Fig. 12B) and phosphorylation of Erk1/2 (MAPK) (Fig. 12C). The fact that IVIg negatively regulates these three pathways suggests that IVIg affects TCR-membrane proximal event. Thus, I next tested whether IVIg suppressed the activation of a TCR-membrane proximal kinase ZAP-70. IVIg co-stimulation inhibited the phosphorylation of ZAP-70 (Fig. 13).

To deeper analyze signaling event that IVIg acts directly on T cells and

suppresses their activation, IVIg-treated T cell lysates were applied to immunoprecipitation using anti-phosphotyrosine antibody (4G10). IVIg co-stimulation induced phosphorylation of 55 kDa protein (Fig. 14). Futhermore, the immunoprecipitates contained tyrosine-phosphorylated proteins which were specifically increased by IVIg co-stimulation (Fig. 15). Those proteins were observed at 55 kDa (Band 1) and 200 kDa (Band 2) by SDS-PAGE analysis. Protein identification by nano LC-MS/MS showed that Band 1 and 2 contained a ZAP-70 modulator Lck kinase and a Lck modulator phosphatase CD45, respectively (Table 1 and 2).

2.4. Discussion

In this chapter, I revealed that IVIg acted directly on conventional T cells to suppress their activation upon TCR ligation. It is widely accepted that IVIg acts on APC to indirectly suppress T cell activation [54,55,56]. The direct T cell regulatory activity of IVIg shown in this chapter is in marked contrast to those previous reports.

Furthermore, I also found that IVIg inhibited TCR signaling. IVIg negatively regulated the three pathways that constitute TCR signaling (NF-κB, Ca^{2+}-calcineurin-NFAT, and MAPK-AP1 pathways), suggesting that IVIg affects the TCR-proximal signaling events to suppress T cell activation. In fact, IVIg did not suppress T cell proliferation stimulation with PMA and ionomycin which bypass TCR ligation (data not shown). In addition, IVIg co-stimulation inhibited the activation of TCR-proximal ZAP-70 kinase (Fig. 13). Preliminary results of immunoprecipitation by using anti-phosphotyrosine antibody indicated that IVIg induced protein phosphorylation. Those immunoprecipitated proteins contained Lck kinase, CD45 tyrosine phosphatase. Lck is an upstream kinase of ZAP-70 and has both activating (Y394) and inhibitory (Y505) phosphorylation sites. CD45 positively and negatively regulates TCR signaling through dephosphorylation of Lck at Y394 and Y505 [58,59].

Recruitment of CD45 to immunological synapse leads to reset of TCR signaling [60,61]. Besides, dedicator of cytokinesis 8 (DOCK8) was also identified by nano LC-MS/MS analysis of Band 2 (Table 2). DOCK8 is a member of the DOCK family of proteins [62], and it has an essential role in immune synapse formation [63]. In addition, myosin-9 which is a protein identified by nano LC-MS/MS analysis of Band 2 (Table 2) is also required for maturation of the immunological synapse [64]. The fact that molecules associated with immunological synapse formation were identified from IVIg-treated immunoprecipitates (shown in Fig. 13, Band 1 and 2; Table 1 and 2) suggested that the immunosuppressive target of IVIg would be a component of immune synapse. To analyze the role of these molecules on the T cell regulatory activity of IVIg is a vital task for the future.

In addition to the elucidation of the T cell suppression mechanism of IVIg, it is necessary to assess the pathophysiological importance of its immunosuppressive activity. The T cell regulatory activity of IVIg discovered in this chapter is a direct action on conventional T cells. Thus, to test whether IVIg suppresses T cell-driven pathologies such as allograft rejection or type 1 diabetes through its direct inhibition of T cell activation would be a suitable trial model.

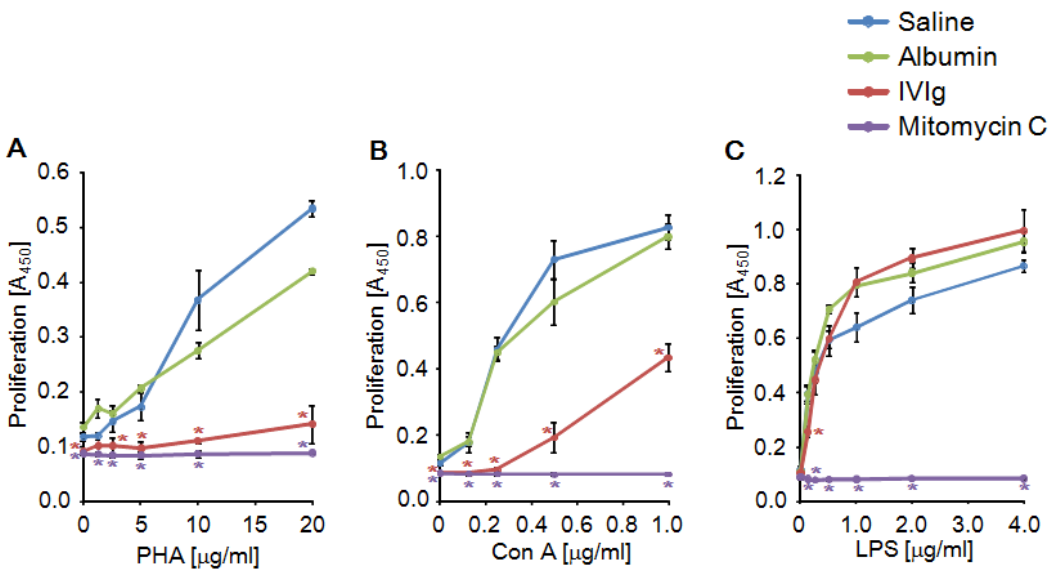

Fig. 7 ***IVIg suppresses proliferation of T cells stimulated by T cell-tropic stimulants.*** **A, B, C** IVIg suppressed proliferation of splenocytes stimulated with PHA (A) and Con A (B), but not that of splenocytes stimulated with LPS (C). Murine splenocytes were cultured with PHA, Con A or LPS and co-stimulated with IVIg (10 mg/ml), albumin (10 mg/ml), mitomycin C (50 μg/ml), or saline. Cell proliferation was measured by BrdU incorporation. *Significantly different at $p < 0.05$ among saline, human albumin, IVIg, and mitomycin C by non-repeated ANOVA and the post hoc Tukey test. Data are presented as means ± SD (n = 3).

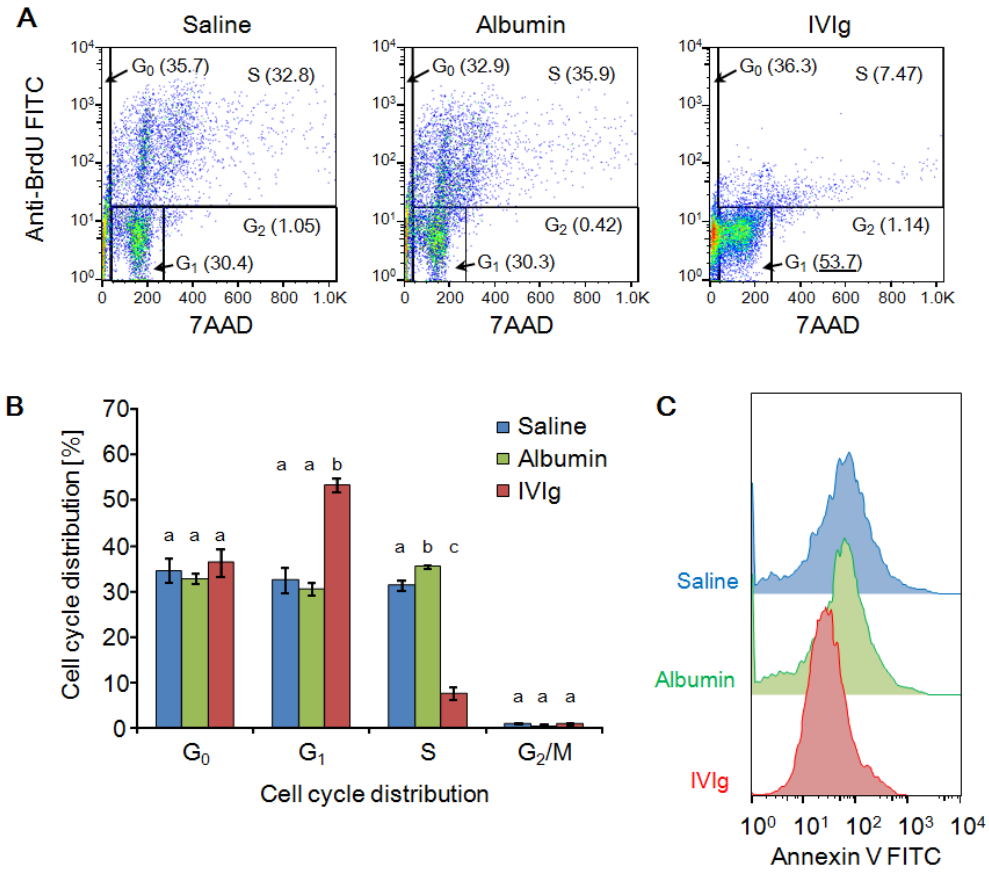

Fig. 8 IVIg induces G_1 cell cycle arrest of T cells, but not apoptosis. **A** IVIg induced G_1 cell cycle arrest of T cells. Murine suplenocyts were cultured with PHA and co-stimulated with IVIg (10 mg/ml), albumin (10 mg/ml) or saline. The cultured splenocytes were labeled with APC-conjugated anti-CD3 antibody, and co-stained with anti-BrdU antibody in BrdU Flow Kit. $CD3^+$ T cells were analyzed by a flow cytometer. **B** Cell cycle distribution of $CD3^+$ T cells cultured with saline, albumin, or IVIg. Bars labeled a-c indicate statistically significant differences among the cell cycle distributions ($p < 0.05$ by non-repeated ANOVA with post hoc Tukey test). Data are presented as means ± SD (n = 3). **C** IVIg failed to induce apoptosis of T cells. Whole suplenocytes were cultured with PHA and co-stimulated with IVIg (10 mg/ml), albumin or saline. The cultured cells were labeled with APC-conjugated anti-CD3 antibody, and co-stained with FITC-conjugated Annexin V. $CD3^+$ T cells were analyzed by a flow cytometer.

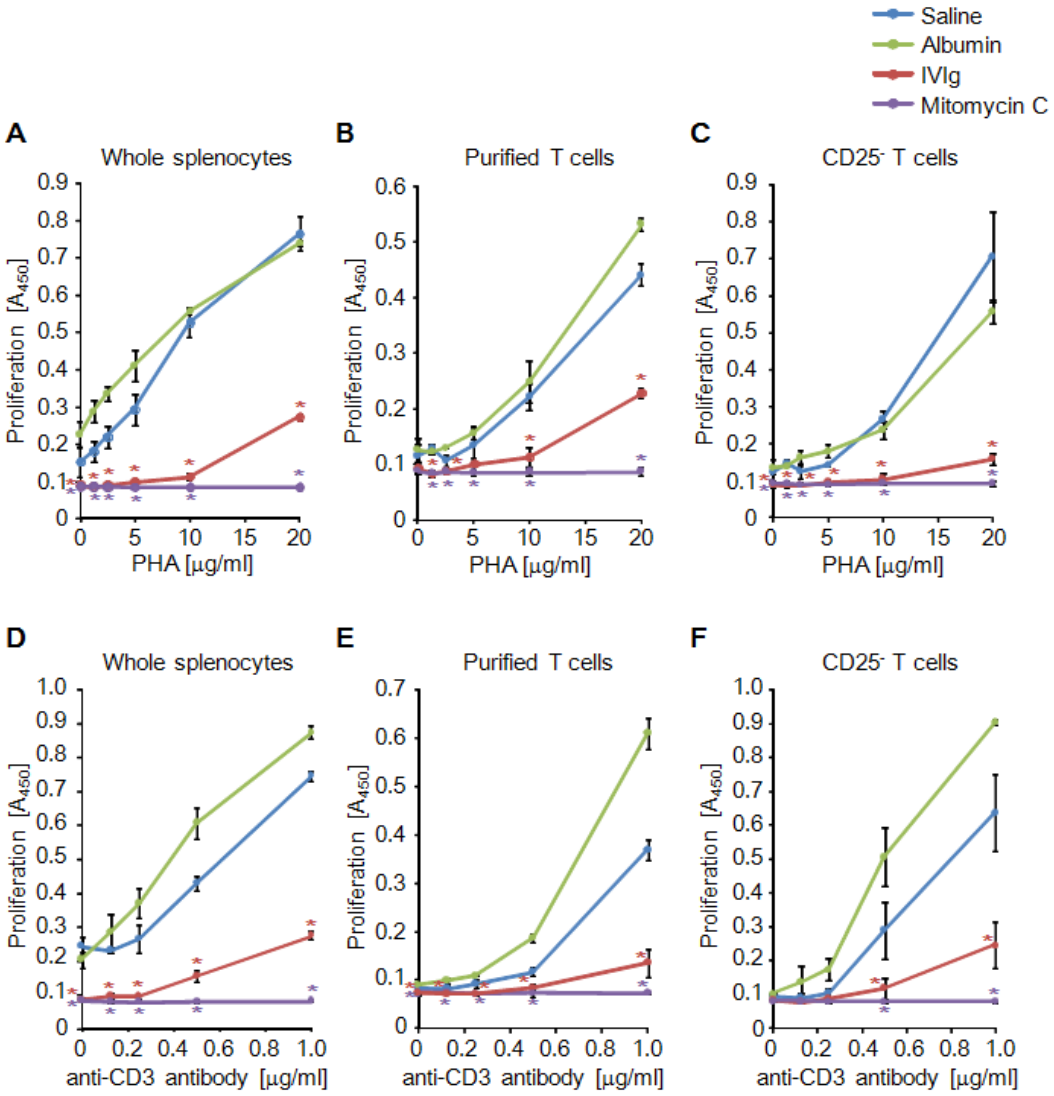

Fig. 9 IVIg suppresses proliferation of purified T cells and CD25$^-$ T cells. **A, D** IVIg suppressed proliferation of whole splenocytes upon stimulation with PHA (A) or anti-CD3 antibody (D). Whole splenocytes were cultured with PHA and anti-CD3 antibody and co-stimulated with IVIg (10 mg/ml), albumin (10 mg/ml), mitomycin C (50 μg/ml), or saline. Cell proliferation was measured by BrdU incorporation. *Significantly different at $p < 0.05$ among saline, albumin, IVIg, and mitomycin C by non-repeated ANOVA and the post hoc Tukey test. Data are presented as means ± SD (n = 3).

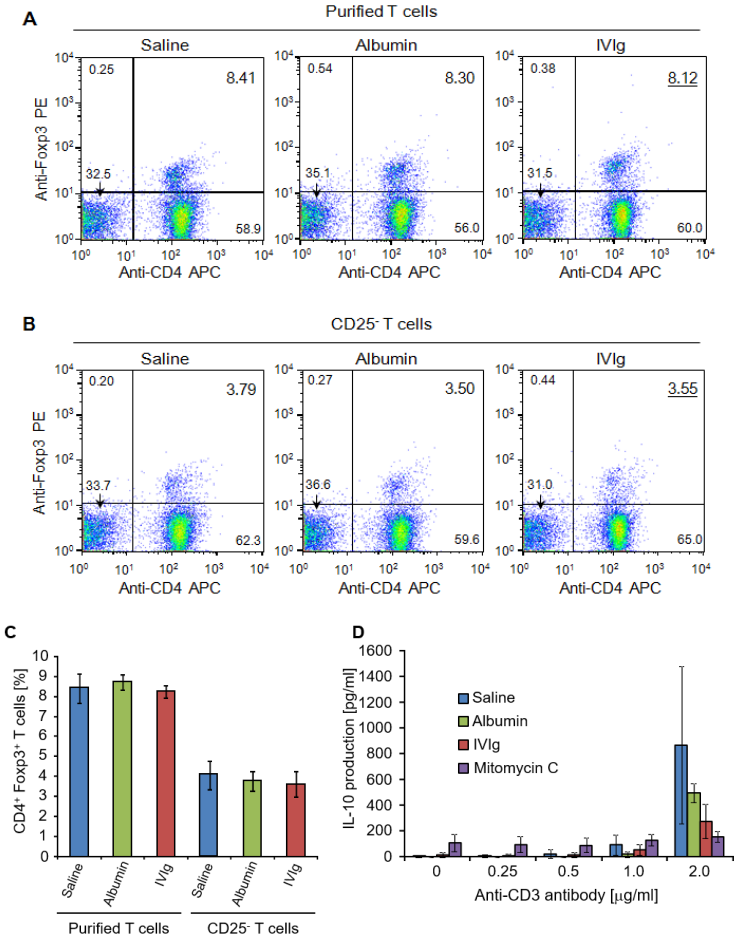

Fig. 10 IVIg does not expand Treg. **A, B** IVIg failed to expand Treg cells. Purified T cells (A) or $CD25^-$ Tcells (B) were cultured with anti-CD3 antibody and co-stimulated with IVIg (10 mg/ml), albumin (10 mg/ml), or saline. Cultured T cells were stained with APC-conjugated anti-CD4 antibody and incubated with Foxp3/Transcription Factor Stain Buffer to co-stain PE-conjugated anti-Foxp3 antibody. Stained T cells were analyzed by a flow cytometer. **C** Rate of $CD4^+$ $Foxp3^+$ Treg in cultured T cells. No significantly different at $p > 0.05$ among saline, albumin, IVIg, and mitomycin C by non-repeated ANOVA and the post hoc Tukey test. Data are presented as means ± SD (n = 3). **D** IVIg did not induce production of IL-10 from T cells. Purified T cells were cultured with anti-CD3 antibody and co-stimulated with IVIg (10 mg/ml), albumin (10 mg/ml), or saline. Produced IL-10 in the supernatant was quantified by ELISA. No significantly different at $p > 0.05$ among saline, albumin, IVIg, and mitomycin C by non-repeated ANOVA and the post hoc Tukey test. Data are presented as means ± SD (n = 3).

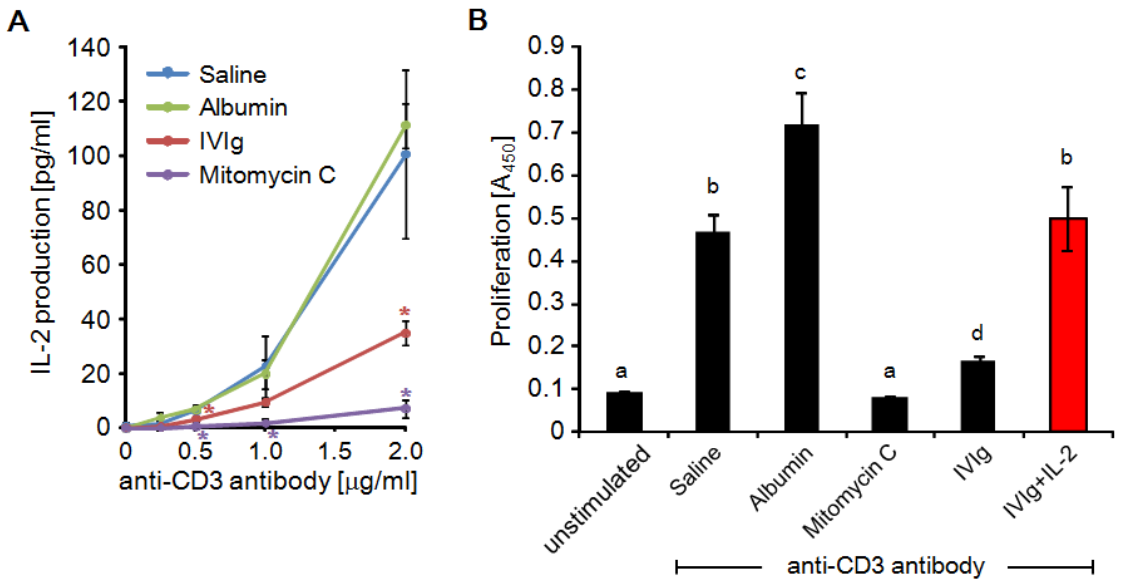

Fig. 11 IVIg suppresses IL-2 production from purified T cells, and its suppressive activity was canceled by adding of exogenous recombinant IL-2. **A** IVIg suppressed IL-2 production from purified T cells. Purified T cells were cultured with anti-CD3 antibody and co-stimulated with IVIg (10 mg/ml), albumin (10 mg/ml), mitomycin C (50 μg/ml) or saline. Produced IL-2 in the supernatant was quantified by ELISA. **B** Exogenous recombinant IL-2 abrogated IVIg's suppressive activity on T cell proliferation. Recombinant IL-2 (250 pg/ml) was exogenously added to T cells stimulated with anti-CD3 antibody (2 μg/ml) and IVIg (10 mg/ml). Cell proliferation was measured by BrdU incorporation. Bars labeled a-d indicate statistically significant differences among the cell cycle distributions ($p < 0.05$ by non-repeated ANOVA with post hoc Tukey test). Data are presented as means ± SD (n = 3).

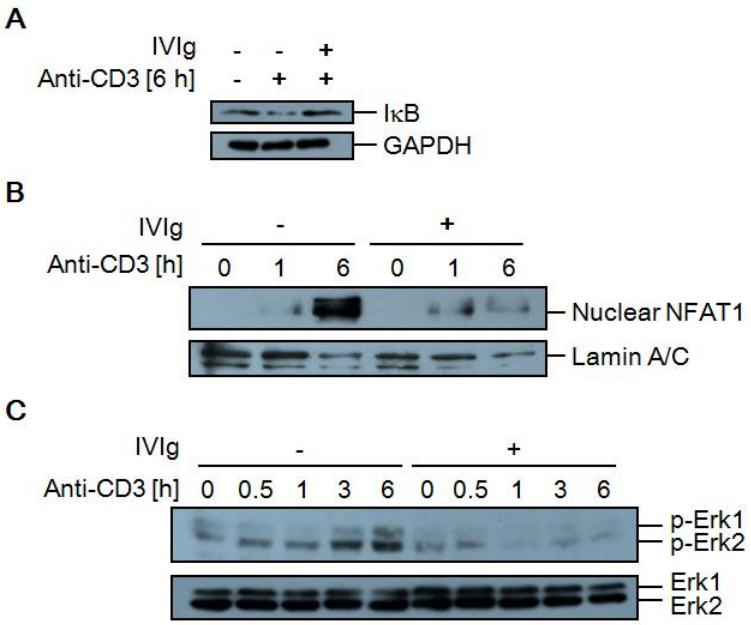

Fig. 12 IVIg negatively regulated TCR signaling. **A B C** IVIg impaired IκB degradation (A), translocation of NFAT1 (B), and phosphorylation of Erk (C). Purified T cells were cultured with anti-CD3 antibody and co-stimulated with or without IVIg for 0, 0.5, 1, 3, or 6 h. Proteins from cultured T cells were fractionated by SDS-PAGE, and then transferred to PVDF membrane. IκB, GAPDH, NFAT1, Lamin A/C, p-Erk1/2, and Erk1/2 were detected by western blotting.

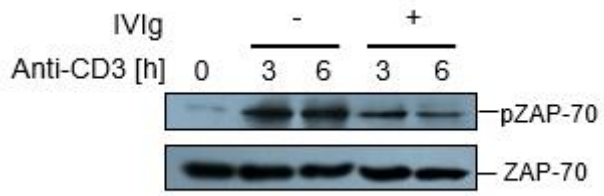

Fig. 13 IVIg inhibited the phosphorylation of a TCR-membrane proximal kinase ZAP-70. Purified T cells were cultured with anti-CD3 antibody and co-stimulated with or without IVIg for 0, 3, or 6 h. Proteins from cultured T cells were fractionated by SDS-PAGE, and then transferred to PVDF membrane. ZAP-70 and pZAP-70 were detected by western blotting.

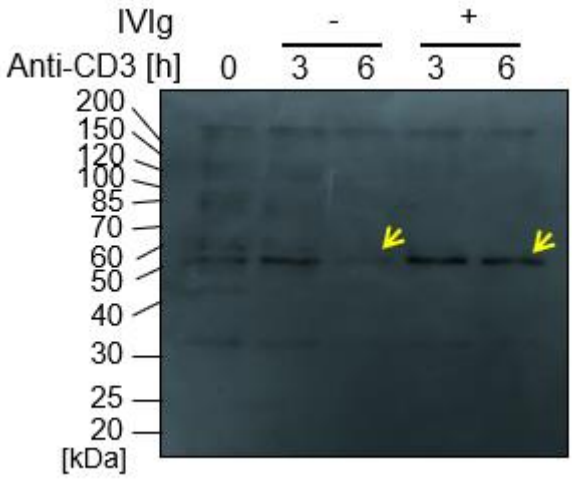

Fig. 14 IVIg co-stimulation induced tyrosine phosphorylation of 55 kDa proteins. Purified T cells were cultured with anti-CD3 antibody and co-stimulated with or without IVIg for 0, 3, or 6 h, and whole T cell lysates were applied to immunoprecipitation using anti-phosphotyrosine antibody. Immunoprecipitates were fractionated by SDS-PAGE, and then transferred to PVDF membrane. Tyrosine-phosphorylated proteins were detected by western blotting using anti-phosphotyrosine antibody.

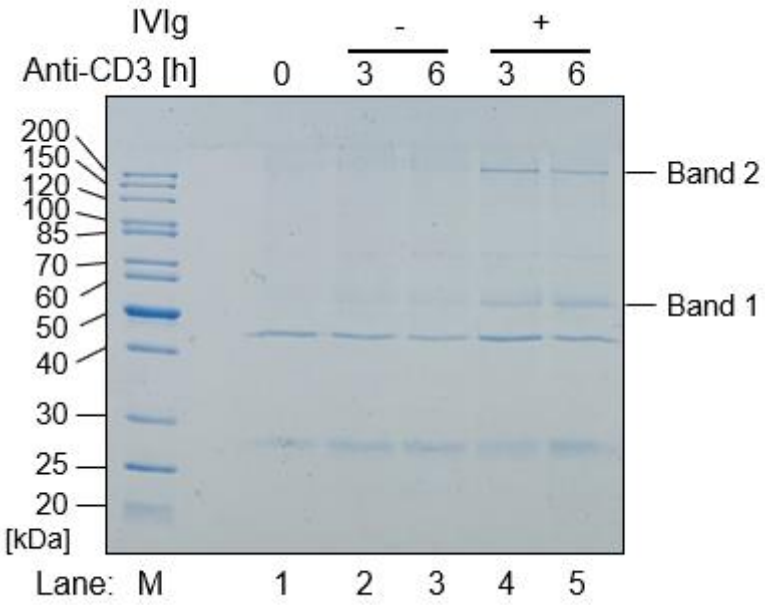

Fig. 15 IVIg-treated immunoprecipitates specifically contained 55 and 200 kDa proteins. Purified T cells were cultured with anti-CD3 antibody and co-stimulated with or without IVIg for 0, 3, or 6 h, and whole T cell lysates were applied to immunoprecipitation using anti-phosphotyrosine antibody. Immunoprecipitates were fractionated by SDS-PAGE, and visualized by coomassie brilliant blue staining.

Table 1. Protein identification of 55 kDa immunoprecipitates by nano LC-MS/MS analysis (Band 1)

Accession	Description	Coverage [%]	Unique Peptides	MW [kDa]	calc. pI	Score Mascot
P56480	ATP synthase subunit beta, mitochondrial OS=Mus musculus OX=10090 GN=Atp5f1b PE=1 SV=2	45	18	56.3	5.34	895
P68372	Tubulin beta-4B chain OS=Mus musculus OX=10090 GN=Tubb4b PE=1 SV=1	55	6	49.8	4.89	561
P99024	Tubulin beta-5 chain OS=Mus musculus OX=10090 GN=Tubb5 PE=1 SV=1	45	4	49.6	4.89	528
Q03265	ATP synthase subunit alpha, mitochondrial OS=Mus musculus OX=10090 GN=Atp5f1a PE=1 SV=1	35	18	59.7	9.19	586
Q8K4G5	Actin-binding LIM protein 1 OS=Mus musculus OX=10090 GN=Ablim1 PE=1 SV=1	22	16	96.7	8.63	521
P68373	Tubulin alpha-1C chain OS=Mus musculus OX=10090 GN=Tuba1c PE=1 SV=1	34	5	49.9	5.1	351
Q922U2	Keratin, type II cytoskeletal 5 OS=Mus musculus OX=10090 GN=Krt5 PE=1 SV=1	19	7	61.7	7.75	354
P68368	Tubulin alpha-4A chain OS=Mus musculus OX=10090 GN=Tuba4a PE=1 SV=1	27	3	49.9	5.06	280
Q61029	Lamina-associated polypeptide 2, isoforms beta/delta/epsilon/gamma OS=Mus musculus OX=10090 GN=Tmpo PE=1 SV=4	32	10	50.3	9.45	327
P06240	**Proto-oncogene tyrosine-protein kinase LCK OS=Mus musculus OX=10090 GN=Lck PE=1 SV=4**	**23**	**8**	**57.9**	**5.25**	**222**
P60710	Actin, cytoplasmic 1 OS=Mus musculus OX=10090 GN=Actb PE=1 SV=1	27	9	41.7	5.48	249
Q62191	E3 ubiquitin-protein ligase TRIM21 OS=Mus musculus OX=10090 GN=Trim21 PE=1 SV=1	19	7	54.1	7.08	228
P02535	Keratin, type I cytoskeletal 10 OS=Mus musculus OX=10090 GN=Krt10 PE=1 SV=3	11	5	57.7	5.11	299
Q9WUM4	Coronin-1C OS=Mus musculus OX=10090 GN=Coro1c PE=1 SV=2	19	8	53.1	7.08	188

(Table 1., continued)

O89053	Coronin-1A OS=Mus musculus OX=10090 GN=Coro1a PE=1 SV=5	25	10	51	6.48	101
P70429	Ena/VASP-like protein OS=Mus musculus OX=10090 GN=Evl PE=1 SV=2	11	4	44.3	8.85	162
Q3TTY5	Keratin, type II cytoskeletal 2 epidermal OS=Mus musculus OX=10090 GN=Krt2 PE=1 SV=1	7	3	70.9	8.06	165
Q6IFZ6	Keratin, type II cytoskeletal 1b OS=Mus musculus OX=10090 GN=Krt77 PE=1 SV=1	8	2	61.3	8.02	189
O35737	Heterogeneous nuclear ribonucleoprotein H OS=Mus musculus OX=10090 GN=Hnrnph1 PE=1 SV=3	14	2	49.2	6.3	133
P70333	Heterogeneous nuclear ribonucleoprotein H2 OS=Mus musculus OX=10090 GN=Hnrnph2 PE=1 SV=1	11	1	49.2	6.3	124

Proteins contained in Band 1 (shown in Fig. 13, Lane 5) were digested by trypsin, and resultant peptide mixture was analyzed by nano LC-MS/MS analysis. Identification of proteins was performed with Proteome Discoverer v2.2 and Mascot. Top 20 proteins identified by Mascot are shown in this table.

Table 2. Protein identification of 200 kDa immunoprecipitates by nano LC-MS/MS analysis (Band 2)

Accession	Description	Coverage [%]	Unique Peptides	MW [kDa]	calc. pI	Score Mascot
Q8VDD5	Myosin-9 OS=Mus musculus OX=10090 GN=Myh9 PE=1 SV=4	69	170	226.2	5.66	10756
P06800	**Receptor-type tyrosine-protein phosphatase C (CD45) OS=Mus musculus OX=10090 GN=Ptprc PE=1 SV=4**	**19**	**21**	**144.7**	**5.94**	**508**
Q8C147	Dedicator of cytokinesis protein 8 OS=Mus musculus OX=10090 GN=Dock8 PE=1 SV=4	11	19	238.8	6.96	509
Q8K4L3	Supervillin OS=Mus musculus OX=10090 GN=Svil PE=1 SV=1	10	15	243	6.87	557
Q62261	Spectrin beta chain, non-erythrocytic 1 OS=Mus musculus OX=10090 GN=Sptbn1 PE=1 SV=2	8	12	274.1	5.58	405
P01867	Ig gamma-2B chain C region OS=Mus musculus OX=10090 GN=Igh-3 PE=1 SV=3	20	6	44.2	6.52	162
P02535	Keratin, type I cytoskeletal 10 OS=Mus musculus OX=10090 GN=Krt10 PE=1 SV=3	11	5	57.7	5.11	284
P16546	Spectrin alpha chain, non-erythrocytic 1 OS=Mus musculus OX=10090 GN=Sptan1 PE=1 SV=4	5	10	284.4	5.33	152
Q8BTM8	Filamin-A OS=Mus musculus OX=10090 GN=Flna PE=1 SV=5	3	6	281	6.04	128
Q922U2	Keratin, type II cytoskeletal 5 OS=Mus musculus OX=10090 GN=Krt5 PE=1 SV=1	12	3	61.7	7.75	150
Q3TTY5	Keratin, type II cytoskeletal 2 epidermal OS=Mus musculus OX=10090 GN=Krt2 PE=1 SV=1	6	2	70.9	8.06	184
Q6P4T2	U5 small nuclear ribonucleoprotein 200 kDa helicase OS=Mus musculus OX=10090 GN=Snrnp200 PE=1 SV=1	3	5	244.4	6.06	92
P04104	Keratin, type II cytoskeletal 1 OS=Mus musculus OX=10090 GN=Krt1 PE=1 SV=4	5	2	65.6	8.15	181
Q61781	Keratin, type I cytoskeletal 14 OS=Mus musculus OX=10090 GN=Krt14 PE=1 SV=2	8	1	52.8	5.17	192

(Table 2., continued)

P03987	Ig gamma-3 chain C region OS=Mus musculus OX=10090 PE=1 SV=2	11	3	43.9	7.14	119
Q6IFZ6	Keratin, type II cytoskeletal 1b OS=Mus musculus OX=10090 GN=Krt77 PE=1 SV=1	8	1	61.3	8.02	148
Q6IFX2	Keratin, type I cytoskeletal 42 OS=Mus musculus OX=10090 GN=Krt42 PE=1 SV=1	8	2	50.1	5.16	163

Proteins contained in Band 2 (shown in Fig. 13, Lane 5) were digested by trypsin, and resultant peptide mixture was analyzed by nano LC-MS/MS analysis. Identification of proteins was performed with Proteome Discoverer v2.2 and Mascot. Top 20 proteins identified by Mascot are shown in this table.

General conclusions

IVIg therapy is a beneficial treatment for autoimmune and severe infectious disorders. However, its immunosuppressive mechanisms remain unclear. To elucidate the therapeutic mechanisms of IVIg would provide valuable drug targets on the treatment of chronic and acute inflammatory diseases, and the molecular targeted drugs that mimic the therapeutic effects of IVIg would be more effective and safer treatment for these diseases. In this thesis, I aimed to redefine and elucidate the target cell subsets and immunosuppressive mechanisms of IVIg based on a hypothesis that IVIg fulfills its immunosuppressive activities through multiple cell targets and molecular mechanisms.

In this study, I discovered two novel immunosuppressive roles of IVIg. First, I demonstrated that IVIg acted on steady-state B cells and suppressed their homeostatic expansion accompanied with B cell aggregation (chapter 1). These B cell regulatory effects are novel activity of IVIg that have not been reported previously, and present results suggest that IVIg can suppress dysregulation of B cell homeostasis leading to chronic inflammation. Dysregulation of B cell homeostasis provokes over production of autoantibodies, and autoimmune diseases characterized by production of multiple

autoantibodies is higher prevalence in women than man [46]. B cell activating factor (BAFF) and female sex hormones (e.x., estrogen and prolactin) contribute above-mentioned B cell-driven pathologies [39,40,41,48,49], and would be the responsible factors for homeostatic expansion of B cells. To evaluate the participation of these molecules to homeostatic expansion of B cells would be provide insights into identification of the B cell regulatory mechanism by IVIg. Second, I showed that IVIg acted directly on conventional T cells and suppressed their activation (chapter 2). Previous studies suggested that IVIg acted APC and then expanded Treg to suppress the activation of conventional T cells. In contrast, present results indicated that IVIg could directly suppress the activation of conventional T cells. These findings are in marked contrast to previous reports. Furthermore, I also found that IVIg negatively regulated the three pathways that constitute TCR signaling (NF-κB, Ca^{2+}-calcineurin-NFAT, and MAPK-AP1 pathways), suggesting that IVIg suppressed TCR-membrane proximal signaling event. In fact, I revealed that IVIg inhibited the activation of a TCR-membrane proximal kinase ZAP-70. In my preliminary experiments, I showed that the immunoprecipitates that immunoprecipitated by anti-phosphotyrosine antibody contained a ZAP-70 modulator Lck kinase and a Lck modulator phosphatase CD45. To analyze the role of these molecules on the T cell regulatory activity of IVIg is an

intriguing trial for the future to fully understand immunosuppressive mechanism of IVIg. Taken together, these results indicate that IVIg acts on different immune cells depending on the immune activation state and fulfills its versatile immunosuppressive capacity by inhibition of the activation of target cells. Autoimmune disorders have a variety of inflammatory conditions caused by versatile pathogenic immune cells. The B and T cell regulatory activities of IVIg discovered in this thesis would provide valuable drug targets on the treatment of chronic and acute inflammatory disorders.

In recent years, the relationship between aging and inflammation has been elucidated [65]. Chronic inflammation is observed not only in rare intractable diseases, but also in age-related diseases such as type 2 diabetes, Alzheimer's disease and neurodegenerative diseases [65]. To elucidate the versatile immunosuppressive mechanism of IVIg would be an important basic research in the development of treatments for age-related inflammatory diseases as well as intractable diseases. In the future, Japan will become a super-aging society, and the development of treatments for age-related diseases is indispensable. IVIg therapy, which is used only in limited treatment of intractable diseases, has the potential to provide immunosuppressive drug targets that contribute to the development of treatments for a wide range of inflammatory diseases.

Acknowledgments

This thesis study has been carried out at the Molecular Biochemistry Laboratory, Department of Molecular Biotechnology, Graduate School of Advanced Science of Matter, Hiroshima University.

I am deeply grateful to Prof. Seiji Kawamoto and Dr. Takashi Fujimura, who give me insightful comments and suggestions throughout this study. I also want to thank Prof. Tsunehiro Aki and Prof. Akio Kuroda for their advice on my doctoral thesis. Meticulous comments of Dr. Miyako Nakano and Prof. Kazuhisa Ono (Emeritus Professor, Hiroshima University) were also an enormous help to me. I thank Tomoko Amimoto (the Natural Science Center for Basic Research and Development, Hiroshima University) for her technical support on nano LC-MS/MS analysis. I would like to offer my special thanks to my laboratory members, who give me warm encouragements and supports.

I am a recipient of a JSPS Research Fellowship for Young Scientists (DC2). This work was supported by JSPS KAKENHI Grant Number JP19J10257.

Finally, I would like to express my gratitude to my family, who give me a chance to chase my dream.

References

[1] A.F. Barahona Afonso, C.M. Joao, The Production Processes and Biological Effects of Intravenous Immunoglobulin, Biomolecules 6 (2016) 15.

[2] A.W. Zuercher, R. Spirig, A. Baz Morelli, F. Kasermann, IVIG in autoimmune disease - Potential next generation biologics, Autoimmun Rev 15 (2016) 781-785.

[3] V.B. E., Untersuchungen ueber das Zustandekommen der Diphtherie-Immunitat bei Thieren (in Germany), Dtsch. Med. Wochenschr. 16 (1890) 1145-1148.

[4] V.B. E., K. S., Ueber das Zustandekommen der Diphtherie-Immunitat und der Tetanus-Immunitat bei Thieren (in Germany), Dtsch. Med. Wochenschr. 16 (1890) 1113-1114.

[5] O.C. Bruton, Agammaglobulinemia, Pediatrics 9 (1952) 722-728.

[6] P. Imbach, S. Barandun, C. Baumgartner, A. Hirt, F. Hofer, H.P. Wagner, High-dose intravenous gammaglobulin therapy of refractory, in particular idiopathic thrombocytopenia in childhood, Helv Paediatr Acta 36 (1981) 81-86.

[7] L. Wang, F.S. Wang, M.E. Gershwin, Human autoimmune diseases: a comprehensive update, J Intern Med 278 (2015) 369-395.

[8] M.R. Arbuckle, M.T. McClain, M.V. Rubertone, R.H. Scofield, G.J. Dennis, J.A. James, J.B. Harley, Development of autoantibodies before the clinical onset of systemic lupus erythematosus, N Engl J Med 349 (2003) 1526-1533.

[9] R. Jonsson, E. Theander, B. Sjostrom, K. Brokstad, G. Henriksson, Autoantibodies present before symptom onset in primary Sjogren syndrome, Jama 310 (2013) 1854-1855.

[10] M.M. Nielen, D. van Schaardenburg, H.W. Reesink, R.J. van de Stadt, I.E. van der

Horst-Bruinsma, M.H. de Koning, M.R. Habibuw, J.P. Vandenbroucke, B.A. Dijkmans, Specific autoantibodies precede the symptoms of rheumatoid arthritis: a study of serial measurements in blood donors, Arthritis Rheum 50 (2004) 380-386.

[11] S. Kotake, N. Udagawa, N. Takahashi, K. Matsuzaki, K. Itoh, S. Ishiyama, S. Saito, K. Inoue, N. Kamatani, M.T. Gillespie, T.J. Martin, T. Suda, IL-17 in synovial fluids from patients with rheumatoid arthritis is a potent stimulator of osteoclastogenesis, J Clin Invest 103 (1999) 1345-1352.

[12] D. Li, B. Guo, H. Wu, L. Tan, C. Chang, Q. Lu, Interleukin-17 in systemic lupus erythematosus: A comprehensive review, Autoimmunity 48 (2015) 353-361.

[13] L.W. Zhang, P.R. Zhou, P. Wei, X. Cong, L.L. Wu, H. Hua, Expression of interleukin-17 in primary Sjogren's syndrome and the correlation with disease severity: A systematic review and meta-analysis, Scand J Immunol 87 (2018) e12649.

[14] A. Waisman, J. Hauptmann, T. Regen, The role of IL-17 in CNS diseases, Acta Neuropathol 129 (2015) 625-637.

[15] L.S. Walker, M. von Herrath, CD4 T cell differentiation in type 1 diabetes, Clin Exp Immunol 183 (2016) 16-29.

[16] H. Kita, Z.X. Lian, J. Van de Water, X.S. He, S. Matsumura, M. Kaplan, V. Luketic, R.L. Coppel, A.A. Ansari, M.E. Gershwin, Identification of HLA-A2-restricted CD8(+) cytotoxic T cell responses in primary biliary cirrhosis: T cell activation is augmented by immune complexes cross-presented by dendritic cells, J Exp Med 195 (2002) 113-123.

[17] C. Scheinecker, M. Bonelli, J.S. Smolen, Pathogenetic aspects of systemic lupus erythematosus with an emphasis on regulatory T cells, J Autoimmun 35 (2010) 269-275.

[18] K.M. Danikowski, S. Jayaraman, B.S. Prabhakar, Regulatory T cells in multiple sclerosis and myasthenia gravis, J Neuroinflammation 14 (2017) 117.

[19] F.A. Cooles, J.D. Isaacs, A.E. Anderson, Treg cells in rheumatoid arthritis: an update, Curr Rheumatol Rep 15 (2013) 352.

[20] J.W. Newburger, M. Takahashi, J.C. Burns, Kawasaki Disease, J Am Coll Cardiol 67 (2016) 1738-1749.

[21] J.W. Newburger, Kawasaki disease: Medical therapies, Congenit Heart Dis 12 (2017) 641-643.

[22] G. Zandman-Goddard, Y. Levy, Y. Shoenfeld, Intravenous immunoglobulin therapy and systemic lupus erythematosus, Clin Rev Allergy Immunol 29 (2005) 219-228.

[23] R. Sakthiswary, D. D'Cruz, Intravenous immunoglobulin in the therapeutic armamentarium of systemic lupus erythematosus: a systematic review and meta-analysis, Medicine (Baltimore) 93 (2014) e86.

[24] J. Jellusova, L. Nitschke, Regulation of B cell functions by the sialic acid-binding receptors siglec-G and CD22, Front Immunol 2 (2011) 96.

[25] J.F. Seite, D. Cornec, Y. Renaudineau, P. Youinou, R.A. Mageed, S. Hillion, IVIg modulates BCR signaling through CD22 and promotes apoptosis in mature human B lymphocytes, Blood 116 (2010) 1698-1704.

[26] T. Muta, T. Kurosaki, Z. Misulovin, M. Sanchez, M.C. Nussenzweig, J.V. Ravetch, A 13-amino-acid motif in the cytoplasmic domain of Fc gamma RIIB modulates B-cell receptor signalling, Nature 368 (1994) 70-73.

[27] M. Ballow, The IgG molecule as a biological immune response modifier: mechanisms of action of intravenous immune serum globulin in autoimmune and inflammatory disorders, J Allergy Clin Immunol 127 (2011) 315-323.

[28] M.D. Kazatchkine, S.V. Kaveri, Immunomodulation of autoimmune and inflammatory diseases with intravenous immune globulin, N Engl J Med 345 (2001) 747-755.

[29] A. Kessel, R. Peri, T. Haj, A. Snir, G. Slobodin, E. Sabo, I. Rosner, Y. Shoenfeld, E. Toubi, IVIg attenuates TLR-9 activation in B cells from SLE patients, J Clin Immunol 31 (2011) 30-38.

[30] J.F. Seite, T. Guerrier, D. Cornec, C. Jamin, P. Youinou, S. Hillion, TLR9 responses of B cells are repressed by intravenous immunoglobulin through the recruitment of phosphatase, J Autoimmun 37 (2011) 190-197.

[31] V.K. Kuchroo, P.S. Ohashi, R.B. Sartor, C.G. Vinuesa, Dysregulation of immune homeostasis in autoimmune diseases, Nat Med 18 (2012) 42-47.

[32] S.J. Kim, J.H. Won, B cell homeostasis and the development of chronic graft-versus-host disease: implications for B cell-depleting therapy, Leuk Lymphoma 53 (2012) 19-25.

[33] M. Wunsch, C. Hohmann, B. Milles, C. Rostermund, P.V. Lehmann, M. Schroeter, A. Bayas, J. Ulzheimer, M. Maurer, S. Ergun, S. Kuerten, The Correlation between the Virus- and Brain Antigen-Specific B Cell Response in the Blood of Patients with Multiple Sclerosis, Viruses 8 (2016) 105.

[34] A. Pollreisz, A. Assinger, S. Hacker, K. Hoetzenecker, W. Schmid, G. Lang, M. Wolfsberger, B. Steinlechner, E. Bielek, E. Lalla, W. Klepetko, I. Volf, H.J. Ankersmit, Intravenous immunoglobulins induce CD32-mediated platelet aggregation in vitro, Br J Dermatol 159 (2008) 578-584.

[35] Y. Kaneko, F. Nimmerjahn, J.V. Ravetch, Anti-inflammatory activity of immunoglobulin G resulting from Fc sialylation, Science 313 (2006) 670-673.

[36] M. Mitrevski, R. Marrapodi, A. Camponeschi, F.M. Cavaliere, C. Lazzeri, L. Todi, M. Visentini, Intravenous Immunoglobulin and Immunomodulation of B-Cell - in vitro and in vivo Effects, Front Immunol 6 (2015) 4.

[37] P. Bjorck, S. Paulie, B. Axelsson, Interleukin-4-mediated aggregation of anti-IgM-stimulated human B cells: inhibition of aggregation but enhancement of proliferation by antibodies to LFA-1, Immunology 75 (1992) 122-128.

[38] C. Bossen, A. Tardivel, L. Willen, C.A. Fletcher, M. Perroud, F. Beermann, A.G. Rolink, M.L. Scott, F. Mackay, P. Schneider, Mutation of the BAFF furin cleavage site impairs B-cell homeostasis and antibody responses, Eur J Immunol 41 (2011) 787-797.

[39] V.T. Chu, P. Enghard, S. Schurer, G. Steinhauser, B. Rudolph, G. Riemekasten, C. Berek, Systemic activation of the immune system induces aberrant BAFF and APRIL expression in B cells in patients with systemic lupus erythematosus, Arthritis Rheum 60 (2009) 2083-2093.

[40] E. Zollars, J. Bienkowska, J. Czerkowicz, N. Allaire, A.M. Ranger, L. Magder, M. Petri, BAFF (B cell activating factor) transcript level in peripheral blood of patients with SLE is associated with same-day disease activity as well as global activity over the next year, Lupus Sci Med 2 (2015) e000063.

[41] X. Mariette, S. Roux, J. Zhang, D. Bengoufa, F. Lavie, T. Zhou, R. Kimberly, The level of BLyS (BAFF) correlates with the titre of autoantibodies in human Sjogren's syndrome, Ann Rheum Dis 62 (2003) 168-171.

[42] E. Claudio, K. Brown, S. Park, H. Wang, U. Siebenlist, BAFF-induced NEMO-independent processing of NF-kappa B2 in maturing B cells, Nat Immunol 3 (2002) 958-965.

[43] N. Kayagaki, M. Yan, D. Seshasayee, H. Wang, W. Lee, D.M. French, I.S. Grewal, A.G. Cochran, N.C. Gordon, J. Yin, M.A. Starovasnik, V.M. Dixit, BAFF/BLyS receptor 3 binds the B cell survival factor BAFF ligand through a discrete surface loop and promotes processing of NF-kappaB2, Immunity 17 (2002) 515-524.

[44] J. Jellusova, A.V. Miletic, M.H. Cato, W.W. Lin, Y. Hu, G.A. Bishop, M.J. Shlomchik, R.C. Rickert, Context-specific BAFF-R signaling by the NF-kappaB and PI3K pathways, Cell Rep 5 (2013) 1022-1035.

[45] G. Recalde, T. Moreno-Sosa, F. Yudica, C.A. Quintero, M.B. Sanchez, G.A. Jahn, A.M. Kalergis, J.P. Mackern-Oberti, Contribution of sex steroids and prolactin to the modulation of T and B cells during autoimmunity, Autoimmun Rev 17

(2018) 504-512.

[46] E. Ortona, M. Pierdominici, A. Maselli, C. Veroni, F. Aloisi, Y. Shoenfeld, Sex-based differences in autoimmune diseases, Ann Ist Super Sanita 52 (2016) 205-212.

[47] N. Kanda, K. Tamaki, Estrogen enhances immunoglobulin production by human PBMCs, J Allergy Clin Immunol 103 (1999) 282-288.

[48] J. Correale, M.F. Farez, M.C. Ysrraelit, Role of prolactin in B cell regulation in multiple sclerosis, J Neuroimmunol 269 (2014) 76-86.

[49] M. Dardenne, P.A. Kelly, J.F. Bach, W. Savino, Identification and functional activity of prolactin receptors in thymic epithelial cells, Proc Natl Acad Sci U S A 88 (1991) 9700-9704.

[50] P. Ascenzi, A. Bocedi, M. Marino, Structure-function relationship of estrogen receptor alpha and beta: impact on human health, Mol Aspects Med 27 (2006) 299-402.

[51] C. Bole-Feysot, V. Goffin, M. Edery, N. Binart, P.A. Kelly, Prolactin (PRL) and its receptor: actions, signal transduction pathways and phenotypes observed in PRL receptor knockout mice, Endocr Rev 19 (1998) 225-268.

[52] V. Goffin, N. Binart, P. Clement-Lacroix, B. Bouchard, C. Bole-Feysot, M. Edery, B.K. Lucas, P. Touraine, A. Pezet, R. Maaskant, C. Pichard, C. Helloco, N. Baran, H. Favre, S. Bernichtein, A. Allamando, C. Ormandy, P.A. Kelly, From the molecular biology of prolactin and its receptor to the lessons learned from knockout mice models, Genet Anal 15 (1999) 189-201.

[53] D. Xiong, Y. Du, H.B. Wang, B. Zhao, H. Zhang, Y. Li, L.J. Hu, J.Y. Cao, Q. Zhong, W.L. Liu, M.Z. Li, X.F. Zhu, S.W. Tsao, L.M. Hutt-Fletcher, E. Song, Y.X. Zeng, E. Kieff, M.S. Zeng, Nonmuscle myosin heavy chain IIA mediates Epstein-Barr virus infection of nasopharyngeal epithelial cells, Proc Natl Acad Sci U S A 112 (2015) 11036-11041.

[54] A.S. De Groot, L. Moise, J.A. McMurry, E. Wambre, L. Van Overtvelt, P. Moingeon, D.W. Scott, W. Martin, Activation of natural regulatory T cells by IgG Fc-derived peptide "Tregitopes", Blood 112 (2008) 3303-3311.

[55] B.M. Fiebiger, J. Maamary, A. Pincetic, J.V. Ravetch, Protection in antibody- and T cell-mediated autoimmune diseases by antiinflammatory IgG Fcs requires type II FcRs, Proc Natl Acad Sci U S A 112 (2015) E2385-2394.

[56] J. Trinath, P. Hegde, M. Sharma, M.S. Maddur, M. Rabin, J.M. Vallat, L. Magy, K.N. Balaji, S.V. Kaveri, J. Bayry, Intravenous immunoglobulin expands regulatory T cells via induction of cyclooxygenase-2-dependent prostaglandin E2 in human dendritic cells, Blood 122 (2013) 1419-1427.

[57] R.J. Brownlie, R. Zamoyska, T cell receptor signalling networks: branched, diversified and bounded, Nat Rev Immunol 13 (2013) 257-269.

[58] M.L. Thomas, E.J. Brown, Positive and negative regulation of Src-family membrane kinases by CD45, Immunol Today 20 (1999) 406-411.

[59] U. D'Oro, J.D. Ashwell, Cutting edge: the CD45 tyrosine phosphatase is an inhibitor of Lck activity in thymocytes, J Immunol 162 (1999) 1879-1883.

[60] B.A. Freiberg, H. Kupfer, W. Maslanik, J. Delli, J. Kappler, D.M. Zaller, A. Kupfer, Staging and resetting T cell activation in SMACs, Nat Immunol 3 (2002) 911-917.

[61] R. Varma, G. Campi, T. Yokosuka, T. Saito, M.L. Dustin, T cell receptor-proximal signals are sustained in peripheral microclusters and terminated in the central supramolecular activation cluster, Immunity 25 (2006) 117-127.

[62] J.F. Cote, K. Vuori, Identification of an evolutionarily conserved superfamily of DOCK180-related proteins with guanine nucleotide exchange activity, J Cell Sci 115 (2002) 4901-4913.

[63] C.J. Kearney, K.L. Randall, J. Oliaro, DOCK8 regulates signal transduction events to control immunity, Cell Mol Immunol 14 (2017) 406-411.

[64] S. Kumari, S. Vardhana, M. Cammer, S. Curado, L. Santos, M.P. Sheetz, M.L. Dustin, T Lymphocyte Myosin IIA is Required for Maturation of the Immunological Synapse, Front Immunol 3 (2012) 230.

[65] S. Xia, X. Zhang, S. Zheng, R. Khanabdali, B. Kalionis, J. Wu, W. Wan, X. Tai, An Update on Inflamm-Aging: Mechanisms, Prevention, and Treatment, 2016 (2016) 8426874.

公表論文

(1) Anti-inflammatory intravenous immunoglobulin (IVIg) suppresses homeostatic proliferation of B cells
Ayane Hori, Takashi Fujimura, and Seiji Kawamoto
Cytotechnology, 70, 921-927 (2018).

(2) Intravenous immunoglobulin (IVIg) acts directly on conventional T cells to suppress T cell receptor signaling
Ayane Hori, Takashi Fujimura, Mai Murakami, Jungyeon Park, and Seiji Kawamoto
Biochemical and Biophysical Research Communications, 522, 792-798 (2020).

参考論文

(1) Intake of a fermented plant product attenuates allergic symptoms without changing systemic immune responses in a mouse model of Japanese cedar pollinosis.
Takashi Fujimura, Ayane Hori, Hideto Torii, Shinsuke Kishida, Yoshinori Matsuura, and Seiji Kawamoto
World Allergy Organization Journal, 11, 31-39 (2018).